Interactive comment on “Combining airborne in situ and ground-based lidar measurements for attribution of aerosol layers” by Anna Nikandrova et al.
Anonymous Referee #1
Received and published: 20 February 2018
This is a nice workup of case studies using multiple sources of data (lidar profile measurements, relative humidity from radiosondes, in situ size distributions, and backtrajectory analysis). Although it is somewhat limited in scope, I think the analysis successfully uses these multiple disparate data sources to gain a deeper understanding of the atmospheric layers in the case studies. The figures are informative and well constructed for showing correspondence between different measurement types and for illustrating interesting aspects of the case studies. I recommend publication after addressing a few points.

Response to comments from Anonymous Referee #1

We thank the referee for the constructive comments to help us to improve the manuscript. Below please find our answers to the comments.

Specific comments:

Page 2, line 30. Delete “at higher latitudes”. Smoke aerosol is not limited to high latitudes.
-Deleted as suggested.

Page 4, line 13. “the cross-polarization channel measures the degree of circular polarization”. I think this should probably be reworded. I don’t think just one channel by itself can measure the degree of polarization; it must be compared to another channel.
-Rephrased: the cross-polarization channel measures the degree of circular polarization relative to the combined channel.
A related question: what is the polarization state of the combined channel? That is, does the polarization split occur before or after the Rayleigh-Mie split?
- The polarization split occurs before the Rayleigh-Mie split.

Page 4, line 14. I would have liked to look up the answer to my previous question in the quoted reference (Goldsmith 2016) but it isn’t in the bibliography.
-Added to the bibliography

Page 4, line 24. What is the particle size cut off of the inlet?
-The aerodynamic particle cut off diameter is 5.0 um. (McNaughton, 2007)
Aerosol size distributions in the figures 2,4,7, 9 are now shown until 5 um.

Page 5, line 29-31. Are these quoted sizes radius or diameter?
-Added ‘with diameters’

Page 10, line 11. “aged dust, especially since the low HSRL circular depolarization values suggest more spherical particles”. I am confused by this sentence. Dust, even aged dust, would be expected to be dominated by non-spherical particles. Either I’m misunderstanding the intent of the sentence (in which case, please reword) or else you are suggesting that aged dust would be expected to have spherical depolarization values similar to what’s observed. If that’s the intent, please include more discussion and references to support this idea.
-We suspect that this is a response of aerosol growing rapidly as it moves from very dry air to much moister conditions, supported by the lowering of the depolarization ratio in the same region. This requires some mixing over small vertical length scales between two otherwise stable layers,

otherwise such a signal would be rapidly ‘smeared out’. Additional evidence is required to confirm this hypothesis.
A clause was missing from our sentence. The sentence has been rephrased ‘This thin layer could be either a result of limited small-scale mixing between two layers, that were probably stable, or the result of large-scale transport of smoke or dust; however, we suspect that this is a response of aerosol growing rapidly as it moves from very dry air to much moister conditions, especially since the low HSRL circular depolarization values suggests that particles in this thin layer were relatively spherical’

Figures 1 seems to show enhanced depolarization during the time period selected for the case study (8 April). Any comment about what this might indicate?
-It might be long-range transport of pollution, that is already discussed on p. 7:
‘The second middle layer had a similar size distribution shape for particles smaller than 100 nm but higher concentrations, and displayed the highest concentrations of supermicron particles, even higher than in the BL. The second middle layer also exhibited much more depolarization than the other layers (Fig. 1b), together implying long-range transport of large non-spherical particles’

Lidar ratio can give important insight into aerosol type and therefore would potentially provide another useful clue for analyzing the case studies. Also, there is significant interest in the aerosol lidar community in cataloging lidar ratio for different aerosol scenarios. HSRL measures backscatter and extinction separately and therefore includes lidar ratio. Why not include lidar ratio in Figures 1 and 6 and in the analysis?
- Lidar ratio was outside the scope of this work, but it will be provided to the community in the next papers including data from the whole BAECC campaign, not only from our case studies.

Page 10, line 23 discusses the depth of cumulus clouds. Since these block the laser light, it’s not clear how you estimate the top-heights of these clouds. Please explain.
-The cloud-top height was seen in the cloud radar that operated during the BAECC campaign. The sentence is rephrased: The cloud radar showed that occasional cumulus clouds were formed from 1000 m in altitude and were able to grow to at least 3000 m in altitude by late afternoon.

In the discussion section, please include more discussion of the proposed mechanisms for new particle formation in the particular cases discussed. I realize there are no measurements available to explain this definitively, but I think some more specific discussion of possibilities supported by literature references would be helpful. Specifically, you discuss new particle formation in the boundary layer for case 1 and then use back-trajectory analysis to infer that the airmass originated over the Arctic Ocean.
Does this mean that the new particle formation occurred over the Arctic Ocean? Was this area covered by sea ice? You also suggest that new particle formation occurred in the elevated layer at the same time. What are published mechanisms for new particle production over sea ice and in elevated layers that would be consistent with these observations?
- The NPF described in the manuscript happens in the boreal forest. Air masses coming from the Arctic Ocean (clean area) are known to be good for NPF in Hyytiälä. Tunved et al. (2006) shows not only that NPF in Hyttiälä is preferred in originally clean marine air masses, but that the NPF is initiated soon after this air enters the boreal forest zone.

Tunved, P., Hansson, H. C., Kerminen, V. M., Ström, J., Dal Maso, M., Lihavainen, H., Y. Viisanen, Y., Aalto, P.P., Komppula, M. and Kulmala, M.: High natural aerosol loading over boreal forests. Science, 312(5771), 261-263, 2006.

Other references describing NPF at the station have been added:

Dal Maso, M., Kulmala, M., Riipinen, I., Wagner, R., Hussein, T., Aalto, P. P., and Lehtinen, K. E.: Formation and growth of fresh atmospheric aerosols: eight years of aerosol size distribution data from SMEAR II, Hyytiala, Finland. Boreal Environment Research, 10(5), 323, 2005.

Kulmala, M., Kontkanen, J., Junninen, H., Lehtipalo, K., Manninen, H.E., Nieminen, T., Petäjä, T., Sipilä, M., Schobesberger, S., Rantala, P. and Franchin, A. et al.: Direct observations of atmospheric aerosol nucleation. Science, 339(6122), pp.943-946, 2013.

Typos, etc.
Page 4, line 14. "Goldsmith" misspelled
-Changed
Page 4, line 24. Is this liters per minute? Can the "L" be capitalized? It looks like a "one".
-Changed to L min^{-1}
Page 5, line 14. "for the algorithm" is not clear. Do you mean for the layer-detection algorithm?
-Added as suggested
Page 5, line 18. "most often indicate edges of layers". Fragmented sentence.
-Rephrased: Layers classified with the HSRL were confirmed with the RS measurements, where edges of layers could be seen in changes of specific and relative humidity profiles.
Page 7, line 1. "this layer" is not clear, since you mention four layers. Which layer?
-Changed 'this layer' to 'the BL'.
Table 1. Please explain acronyms in the table caption (particularly "NPF").
-Changed: Acronyms are explained in the table caption.
Also, the formatting of the "MidLII" column is strange in that it is unlike any other column in having both the height and depth. I realize this is to save space since there is only one layer. Another possibility that might be clearer is removing the "MidLII" column and putting two sets of measurements (separated by a comma) in that row of the "MidL height" and "MidL depth" columns.
-Changed as suggested.
Figures 2 and 7, the annotations are hard to read. Repeating the information from the color legend in the caption would help. It would also be useful to indicate the layer boundaries as lines or markers on the humidity profile or lidar curtain so that it would be more immediately obvious where the in situ size distributions are applicable.
- Boundaries are added to the RH plot on fig. 2 and 7 as suggested, and legend is changed, so it can be easier to read.
Also, it would be useful to make the axis labels bigger in Figures 2, 3, 7, 8 and 9.
- Figure axes are already as big as possible to fit text nicely.
There seems to be a rendering or smoothing artifact in the lidar curtain in Figure 2e that shows as a series of horizontal lines where the lidar backscatter profile does not change for 15 or 20 minutes between 11:50 and 12:10.
-Smoothing artefact due to MATLAB plotting issue in data gaps - Fig. 2e now corrected. Data gap was due to calibration period.

The manuscript “Combining airborne in situ and ground based lidar measurements for attribution of aerosol layers” focuses on investigating different layers present in the troposphere up to 3500 m. For this purpose, they combine aerosol particle size distribution data recorded on board of a research airplane with ground-based High Spectral Resolution Lidar (HSRL), radiosonde profiles and air-mass back trajectory analysis within the BAECC campaign which took place in Southern Finland 2014. The data is presented for two main case studies recorded at the same location but with differing meteorological conditions. The presence of several lofted layers was seen and compared to findings from the back trajectory analysis.
I recommend the paper for publication in ACP after the following comments have been addressed:

Response to comments from Anonymous Referee #2

We thank the referee for the constructive comments to help us to improve the manuscript. Below please find our answers to the comments.

Comments:
P4, Chapter 2.1- HSRL: what is the minimum altitude that can be measured?
Added to the text: ‘The HSRL instrument provides profiles from around 50 m up to 30 km in altitude.’

Full overlap between the transmitted laser beam and the telescope is reached at around 3 km, however values below this altitude can be used qualitatively down to the minimum altitude with their uncertainty increasing as the overlap decreases. Note that the retrieved backscatter coefficient and lidar depolarization ratio values are usually less affected by the overlap issue as they are derived by taking ratios of two channels (ie combined and molecular channels, combined and cross polarization channels), assuming all channels follow similar paths in the detection chain.

P4, line 32: What type of RH sensor was employed and what is the expected uncertainty?
Added to the text: a relative humidity sensor (Rotronic HygroClip-S, accuracy 0.8 % at 23 °C)

P5, Chapter 2.2: It is stated that the SMPS data is corrected for elevated RH in the ambient with a certain GF. Is this correction implemented as a function of height, meaning that for each altitude the actual RH that was measured was used to determine the GF?
-Yes. Added to text: The correction for GF was implemented as a function of height for the SMPS data.
What about the influence of elevated RH on the optical properties? It is not stated in the paper which index of refraction was used to determine the optically measured size distribution! As a correction for the SMPS is introduced I would strongly suggest to also apply a correction to changes in the index of refraction of the particles and adjust the actual size range measured by the OPS.
-Index of refraction for water droplets (1.334) was used for OPS measurements.
During Case Study I, the relative humidity values were lower than 50 %, so that any changes in refractive index are expected to be minor. During Case Study II, it is true that RH values were much higher at some altitudes, and that this may induce some changes in the refractive index that is assumed constant for the OPS data. However, we have no chemical composition measurements from the aircraft from which the real refractive index could be determined, hence we may introduce more errors by varying the refractive index. In this study we are more concerned with identifying that there are significant differences in the aerosol size distribution from layer to layer, for which we believe our simple assumption of a single refractive index is still appropriate.

Figures 2&7: Could you add lines for the different layers in the plots depicting the back-scatter cross sections? It is not very clear where the boundaries were chosen.
- Lines were added to the left most panels of figures 2 and 7.
The text was modified: The ambient size distributions were then grouped by similarities in the size distribution and taking into account the layer boundaries found in the HSRL data.

P7, line 9: Where can the mentioned depolarization be seen?
Added to the text: Fig 1b

P8, Chapter 3.1.3: Which data was used for the HYSPLIT trajectories (GDAS etc.?) and what resolution was employed? These two things can have a strong influence on the analysis.
- Added to the text: The National Center for Environmental Prediction (NCEP) Global Data Assimilation System (GDAS) dataset with 1 degree resolution was used for the meteorological input to the model.

P8, line 30: "close to surface" – I am a bit confused by this statement as from Fig. 5d the lowest height visible is around 1000 m, and I would not refer to that as "close to surface". Could you rather state the actual altitude range? Such phrasing is also used later, and I would suggest changing that as well (for blue lines).
-Modified as suggested

P9, lines 12-15: Can some possible reasons for the not-matching altitudes between HYSPLIT and the measurements be pointed out?
- Added to the text: Errors in trajectories (particularly in the vertical) arise from the difficulties that the meteorological models providing the wind fields have in accurately representing vertical motion, turbulence and other sub-grid scale features (Stohl et al., 2001, Riddle et al., 2006, Hoffmann et al., 2016).

Riddle, E. E., P. B. Voss, A. Stohl, D. Holcomb, D. Maczka, K. Washburn, and R. W. Talbot (2006), Trajectory model validation using newly developed altitude□controlled balloons during the International Consortium for Atmospheric Research on Transport and Transformations 2004 campaign, *J. Geophys. Res.*, 111, D23S57, doi:10.1029/2006JD007456.

Stohl, A., L. Haimberger, M. P. Scheele, and H. Wernli. "An intercomparison of results from three trajectory models." *Meteorological Applications* 8, no. 2 (2001): 127-135.

L. Hoffmann, T. Rößler, S. Griessbach, Y. Heng and O. Stein, Lagrangian transport simulations of volcanic sulfur dioxide emissions: Impact of meteorological data products, *Journal of Geophysical Research: Atmospheres*, **121**, 9, (4651-4673), (2016).

P9, line 26+27: What is meant here by "the smaller size range"? I am also confused by the change mentioned for 10th of April. What is it referred to? I cannot see a clear difference between the lines in Fig. 4B?
-This paragraph is rephrased to be clearer: For particles smaller than 300 nm, the shape of the size distribution and the number concentrations changed from day to day.
For particles larger than 300 nm, while the number concentration varied, the shape of the distribution remained similar across all 3 days.

Specific comments: - changed as suggested
P2, line 3: change “vary” to “varies”
P4, line 23: change “stainless tube” to “stainless steel tube”
P5, line 4: change “campaigns” to “campaign”
P5, line 20: add “the” before “Cessna”
P10, line 2: change to “air masses of two different origins and heights intersected. The panels of Fig. 5 demonstrate the
...

I have reviewed “Combining airborne in situ ground based lidar measurements for attribution of aerosol layers” by Nikandrova et al. The work presents a combination of results derived from a range of instrument systems deployed during the BAECC (Biogenic Aerosols Effects on Cloud and Climate) campaign conducted at a field site in southern Finland. The work presents evidence of lofted layers of aerosol and examines differences in the aerosol size distributions, lidar backscatter, and lidar depolarization ratio for two case studies. Overall, the results presented in the manuscript should be interest to the larger research community.
I believe that he manuscript will be acceptable for publication after addressing a few significant concerns.

Response to comments from Anonymous Referee #3

We thank the referee for the constructive comments to help us to improve the manuscript. Below please find our answers to the comments.

1. The work makes a point of using relative humidity (RH) to help define layers and to better understand some of the differences in the observed size distributions. The authors point out that the ambient RH was measured near the aerosol inlet, but there is no discussion of how the RH might change as the particles move through the system. Perhaps the impact is small, but it should be addressed in the manuscript in some fashion. In addition, there is little detail given about the RH measurements themselves (for example, what instrument is used to make the measurements).

Added to the text: a relative humidity sensor (Rotronic HygroClip-S, accuracy 0.8 % at 23 °C)

For the SMPS measurements the change in the RH in the system was not an issue, as the air was dried before aerosol size distribution was measured (already mentioned in the text on p. 5). As for OPS measurements, RH higher than 40% could accelerate hygroscopic growth. Particles spend some tens of seconds in the sampling line. Humidity inside the cabin was lower than outside (higher temperature inside) so hygroscopic growth should have not taken place. Most of our case studies have lower than 50 % ambient humidity.

2. The authors describe that the atmospheric thermodynamic structure is hard to interpret for Case II. Based on the figure derived from the radiosonde, it looks like it could be a more typical profile with clear subcloud layer to an altitude of 750 m, and then a cloud layer from 750 m to approximately 1700 m. It could be helpful to examine the potential temperature profile in addition to the humidity in this case.

We have now examined the potential temperature, and we still think that the thermodynamic structure during this day was not easy to interpret. As seen from the profile, there are no clear sublayer boundaries:

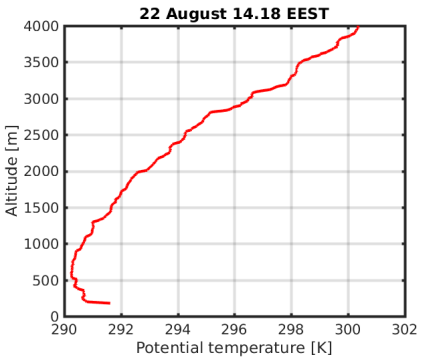

Minor comments:
1. Page 1, line 14: The acronym DOE (rather than DoE) is generally used for the Department of Energy
-Changed as suggested to DOE

2. Page 1, line 17 (and other locations): The terms “low” and “high” are used throughout the manuscript when referring to variability, aerosol concentration, and other meteorological variables. It is better usage to use “small” and “large” unless one is referring to differences related to altitude.
-Changed as suggested from ‘low/high’ to ‘small/large’ for the term variability (page 1, 8, 12). We think ‘low/high’ is appropriate to use for aerosol concentration.

3. Page 2,line 15. The authors might want to consider adding a reference to Wang et al. (2016), a Nature paper also looking at vertical transport of aerosol.
-Added suggested reference

4. Page 3, lines 2-6. Muller etal. (2014, AMT) also showed comparisons of aerosol microphysical properties derived from HSRL with in situ data.
-Added suggested reference

5. Page 2, line 20. Suggest using “aerosol” or “particles” rather than “aerosol particles”.
-We think “aerosol particles” is the best word to use when discussing aerosol particles in this case.

6. Page 5, line 16. Does the reference to BLs really mean convective BLs or all Bls?
- The reference is to all BLs, and on a clear day the BL is usually convective.

7. Page 5, lin3 24. The manuscript cites the work of Laakso et al. (2004). Are their results for the same geographic area?
-Yes, they are. Added to the text: a growth factor (GF) calculated for a boreal forest environment using measurements from SMEAR II station.

8. Page 6 (figure 1). The humidity profiles in the figure are hard to interpret due to the lack of a scale. Is there a way to add a scale or axes that would not make the figure too hard to read?
-Figure 1 was intended to show the general overview of the situation during three days, while humidity profiles for case studies could be seen on Figure 2 with scales.

9. Page 6. line 21. It is not clear to me how you determined the interface zone, and what you really mean by the term. It is addressed a bit later in the manuscript, but some additional explanation here would be helpful when the term is introduced.
-Added to the text: The interface zone was a shallow zone situated at the boundary between two more substantial layers and was characterized by large backscatter values and depolarization values different from the surroundings. No corresponding thin layer was detected in the humidity profiles, whether from the radiosonde or aircraft.

10. Page 7 (and Figure 2 and 7). Is there a way to mark the specific layers on the plots of aerosol backscatter? I know that there is a table, but it could be helpful to add the information to the figure (assuming that the figure remains legible).
-Specific layer boundaries were added to the RS profiles panels of Figures 2 and 7.

11. Page 8, lines 4-5. Should a reference or references for NPF be added?
-Added references:

Dal Maso, M., Kulmala, M., Riipinen, I., Wagner, R., Hussein, T., Aalto, P. P., and Lehtinen, K. E.: Formation and growth of fresh atmospheric aerosols: eight years of aerosol size distribution data from SMEAR II, Hyytiala, Finland. Boreal Environment Research, 10(5), 323, 2005.

Kulmala, M., Kontkanen, J., Junninen, H., Lehtipalo, K., Manninen, H.E., Nieminen, T., Petäjä, T., Sipilä, M., Schobesberger, S., Rantala, P. and Franchin, A. et al.: Direct observations of atmospheric aerosol nucleation. Science, 339(6122), pp.943-946, 2013.

Tunved, P., Hansson, H. C., Kerminen, V. M., Ström, J., Dal Maso, M., Lihavainen, H., Y. Viisanen, Y., Aalto, P.P., Komppula, M. and Kulmala, M.: High natural aerosol loading over boreal forests. Science, 312(5771), 261-263, 2006.

12. Page 8, lines 20-21. I can see how this sentence is needed, but it seems to be just tacked onto the end of the section.
-This sentence is removed, because only aerosol concentrations higher than 0.1 cm^{-3} are shown now on the figure. (This sentence is not needed anymore as it explained large variability in the concentrations below that).

13. Page 10, lines 9-10. How would small scale mixing lead to the behavior that is shown in the figure?
-We suspect that this is a response of aerosol growing rapidly as it moves from very dry air to much moister conditions, supported by the lowering of the depolarization ratio in the same region. This requires some mixing over small vertical length scales between two otherwise stable layers, otherwise such a signal would be rapidly ‘smeared out’. Additional evidence is required to confirm this hypothesis.
The sentence is rephrased: This thin layer could be either a result of limited small-scale mixing between two layers, that were probably stable, or the result of large-scale transport of smoke or dust; however, we suspect that this is a response of aerosol growing rapidly as it moves from very dry air to much moister conditions, especially since the low HSRL circular depolarisation values suggest more spherical particles in this thin layer.

14. Page 11, line 10. Suggest using the same units as shown on the figure.
-We have changed the units as suggested.

15. Page 12, line 2. The text mentions deep convection, but can that be safely said from the data that has been presented so far? Wouldn’t the HSRL have issues seeing the cloud-top height?
-The HSRL does not see the cloud top heights (there is complete attenuation of the signal where there are clouds), but the cloud-top height was seen in the cloud radar that operated during the BAECC campaign.
We do not intend to add a figure showing the radar reflectivity so we have removed ‘deep’.

Anonymous Referee #4
Review of : Combining airbone in-situ and ground based Lidar measurements for attribution for attribution of aerosol layers.
By Nikandrova et al.
The authors describe two case studies (clear sky and cloudy sky) observed over the SMEAR-II station during a field campaign in 2014. The authors used airborne measurements (mostly in-situ size distributions) associated to ground based HSRL Lidar.
This manuscript is of interest for the scientific community but need major revisions before submission to ACPD.

Response to comments from Anonymous Referee #4

We thank the referee for the constructive comments to help us to improve the manuscript. Below please find our answers to the comments.

Fist of all, the aim of the paper is pretty vague: ' investigate aerosol layers in a rural environment' and need to be clarified.
We have tried to clarify the aim of the paper in the introduction and added several sentences: 'We were particularly interested in how the aerosol size distribution varied both within and between layers. This information could be used to determine whether there was mixing within and between layers, and whether there had been any recent contact with the surface.'
We have also added this sentence at the end of the last paragraph of the introduction: 'Back trajectory analysis was conducted for both case studies to examine whether these analyses produced similar layer structures to those observed, and how closely the diagnosed layer altitudes corresponded with those observed by the HSRL.'

This paper is showing size distribution differences that occur within each layer of the atmosphere as a function of time. The authors interpret each increase of the fine particle number concentration as a nucleation event within each layer. However, the differences of Aitken, Accumulation and Coarse number concentrations are only pointed out.
Although we interpret these increases as NPF, we focus on how variable the aerosol size distribution is within each layer, and how the shape of the aerosol size distribution changes over time; this can then be used to infer any mixing within or between layers. The relative lack of mixing observed in elevated layers may then inform likely evolution of aerosol undergoing long-range transport.

The conclusions of this paper needs some work : The comparison of the RH and HSRL profiles with HYSPLITT results are most of the times in good agreement but the ''heights did not always coincide". These height differences are not expressed in the main part of the paper and should probably be. . .
We have added more text to the main part after this sentence 'During 9 and 10 April, for example, the trajectory BL height was lower than the BL seen from the HSRL and consequently, the trajectory analysis suggested a thicker middle layer.', 'BL height diagnosed from trajectory analyses was 50-800 m lower than that observed, whereas for elevated layers, the layer boundary heights were better represented, with departures typically less than 200 m. These larger height differences for layers associated with the BL top are attributed to the difficulties that meteorological models have in representing the BL (e.g. Holtslag et al., 2013), which are then propagated through to the trajectories.'

Added to the conclusion: Errors in trajectories (particularly in the vertical) arise from the difficulties that the meteorological models providing the wind fields have in accurately representing vertical motion and turbulence, the boundary layer, and other sub-grid scale features (Stohl et al., 2001, Riddle et al., 2006, Hoffmann et al., 2016). Uncertainties in the horizontal can be determined using ensemble trajectory techniques (Stohl et al., 2001) but these are less likely to capture vertical discrepancies arising from processes that the meteorological model may not capture correctly, such as the boundary layer.

L. Hoffmann, T. Rößler, S. Griessbach, Y. Heng and O. Stein, Lagrangian transport simulations of volcanic sulfur dioxide emissions: Impact of meteorological data products, *Journal of Geophysical Research: Atmospheres*, **121**, 9, (4651-4673), (2016).

Holtslag, A.A., G. Svensson, P. Baas, S. Basu, B. Beare, A.C. Beljaars, F.C. Bosveld, J. Cuxart, J. Lindvall, G.J. Steeneveld, M. Tjernström, and B.J. Van De Wiel, 2013: Stable Atmospheric Boundary Layers and Diurnal Cycles: Challenges for Weather and Climate Models. Bull. Amer. Meteor. Soc., 94, 1691–1706, https://doi.org/10.1175/BAMS-D-11-00187.1

Riddle, E. E., P. B. Voss, A. Stohl, D. Holcomb, D. Maczka, K. Washburn, and R. W. Talbot (2006), Trajectory model validation using newly developed altitude□controlled balloons during the International Consortium for Atmospheric Research on Transport and Transformations 2004 campaign, *J. Geophys. Res.*, 111, D23S57, doi:10.1029/2006JD007456.

Stohl, A., L. Haimberger, M. P. Scheele, and H. Wernli. "An intercomparison of results from three trajectory models." *Meteorological Applications* 8, no. 2 (2001): 127-135.

A brief presentation of the Hysplitt model and especially the resolution of the data input of the model could help the authors to interpret these differences.
Added to the text: The National Center for Environmental Prediction (NCEP) Global Data Assimilation System (GDAS) dataset with one degree resolution was used for the meteorological input to the model.

Also the last conclusion of the paper is that the synergy between radiosounding, LIDAR and back trajectories gives more confidence in determining the air mass origin. Is this really the main conclusion ?
This is one of the main conclusions, and we have added more text (also written in the comment above: Errors in trajectories (particularly in the vertical) arise from the difficulties that the meteorological models providing the wind fields have in accurately representing vertical motion and turbulence, the boundary layer, and other sub-grid scale features (Stohl et al., 2001, Riddle et al., 2006, Hoffmann et al., 2016). Uncertainties in the horizontal can be determined using ensemble trajectory techniques (Stohl et al., 2001) but these are less likely to capture vertical discrepancies arising from processes that the meteorological model may not capture correctly, such as the boundary layer.)

Last, the authors state: ’Evidence for cloud processing of aerosol particles was also seen in the BL but the amount of processing varied [. . .]’. The authors are showing Hoppel minimum that could be related to cloud processing but it’s not supported by real evidence. It could also be due to different sources of aerosol with one source quite close to the instrumental site ? Moreover, I believe you can’t talk about the ‘amount of processing’. . .
We agree that we have no direct evidence of cloud processing. However, the lower part of the BL was very well-mixed which suggests that any local sources should also be reasonably well-mixed; there is low variation in other size ranges for the entire BL.

This sentence has been reworded: ‘In the BL, the aerosol size distribution displayed a Hoppel minimum suggesting cloud processing of aerosol particles, but with variations that were presumably again due to the specific nature of the updrafts and downdrafts resulting in BL mixing that was not fully homogeneous in the upper part of the BL.’

Minor corrections:

P3 L 4 : Not well said. Please rephrase
Rephrased: ‘Microphysical properties retrieved from HSRL-2 showed a good agreement with in situ measurements; however, backscatter and extinction coefficients calculated from corresponding in situ measurements were consistently underestimated, which was attributed to the undersampling of coarse mode particles by in situ measurements’

Page 3 L15 : Needs to add references to support that like Crumeyrolle et al., 2010; Rose et al., 2015a, Berland et al., 2016.
Rephrased and added two of suggested references: This suggests that, in the boreal forest, large-scale NPF events are typically confined to the BL, similar to results found in other environments (Crumeyrolle et al., 2010; Berland et al., 2016).
Rose et al., 2015a reported NPF events in the free troposphere over Mediterranean.

Figure 2 : You are always refering to the mode you define P5. Could you add on your size distribution plots the limits of each mode (nucleation, Aitken, Accumulation, Coarse). It would help the reader.
Added as suggested

No error bars on the Figure 2i within the small particles range for the middle layer ?
There is no error bar because shaded areas show variability in the layers, and in the middle layer during this flight, small particles were detected only once. This is explained in the text on p. .

P10 L7 : ‘A very high peak’ : could you add in comparison to the rest of the profile ?
Added as suggested

P10 L10 : Smoke or Dust are not known to be spherical particles …
A clause was missing from our sentence. The sentence has been rephrased ‘This thin layer could be either a result of limited small-scale mixing between two layers, that were probably stable, or the result of large-scale transport of smoke or dust; however, we suspect that this is a response of aerosol growing rapidly as it moves from very dry air to much moister conditions, especially since the low HSRL circular depolarization values suggest that particles in this thin layer were relatively spherical.’

P11 L14 : below 100nm instead of 30nm
We left 30 nm as originally written because on the figure 7c aerosol number size distribution in the upper layer (blue) lower than in the first middle layer (yellow) below 30 nm.

P11 L 22 : Please add 100nm to show the reader where the Hoppel minimium is located.
Added as suggested

P12 L17 : around 100nm replace with around 70nm
Replaced as suggested

Figure 7. Not able to distinguish the 3 green shades…
We have changed colours.

Figure 9 : No error bars : Does it mean that you used only one spectra. If yes than it needs to be stated somewhere.
Error bars added to the plot.

5 L25 : Please add explanations. I don't want to read Laakso et al. To understand what you did. The GF is usually dependant of the different compounds present in the aerosol. So how did you get this information ?
Added to the text: 'using a growth factor (GF) calculated for a boreal forest environment using measurements from Hyytiälä station by Laakso et al. (2004). They weighted the GF for compounds with different hygroscopicity according to their respective fractions to obtain an optimal combined GF coefficient.'

P7 L25 : Hard to tell cause there are no measurements of the fine particle number concentration within the middle layer…
No particles smaller than 15 nm were detected in the upper and middle layers during the morning flight even though the detection limit is 10 nm, but these were observed in the afternoon flight, providing evidence for NPF in elevated layers.

P9 L27-29 : Please tell us more about the difference you see cause it's not obvious for me.
This paragraph is rephrased to be clearer: 'For particles smaller than 300 nm, the shape of the size distribution and the number concentrations changed from day to day. For particles larger than 300 nm, while the number concentration varied, the shape of the distribution remained similar across all 3 days.'

P11 L 20 : If you are implying that the cloud base is playing a role in the mixing efficiency be more clearer
We have rephrased this sentence 'Two tendencies are seen in the BL: a more mixed lower part up to about 1000 m where the cloud bases were, and a less mixed upper part' as we did not mean to imply whether cloud base plays a role. It happens that saturation occurs at a similar altitude as the mixing profile begins to depart from a well-mixed profile, but we do not infer that cloud is necessarily the cause of the change in the mixing profile.
Our sentence now reads 'The BL was well-mixed up to 600 m, and became progressively less well mixed above this, with convectively buoyant air parcels reaching up to 2500 m. The radiosonde thermodynamic profile suggested that deep convection to 4 km or so was possible, and did indeed occur later on in the day.'

P12 L 19 : Any interpretation why there is less particles above 500nm ?
Added to the text: This may due to dilution as the growing BL entrains air from above with lower concentrations in this size range.

P12 L22 : Do you mean that nucleation occurs over the cloud top ? Please add references to support this.
With cloud-driven entrainment we are only implying that there might be localized mixing, rather than a fully-mixed layer. Hence, there may be pockets with slightly higher and slightly lower concentrations, without NPF necessarily occurring.

Section 3.1.2 : If you are talking about erors you need to state the number of SD you used to get the average showed in figure 2. ..
We report uncertainties using one standard deviation, as written in the caption for the figures and in the text.

Combining airborne in situ and ground-based lidar measurements for attribution of aerosol layers

Anna Nikandrova[1], Ksenia Tabakova[1], Antti Manninen[1], Riikka Väänänen[1], Tuukka Petäjä[1], Markku Kulmala[1], Veli-Matti Kerminen[1] and Ewan O'Connor[2]

[1]~~University of Helsinki, Department of Physics P.O. Box 64, FIN-00014, Finland~~

[1]Institute for Atmospheric and Earth System Research / Physics, Faculty of Science, University of Helsinki, Finland

[2]Finnish Meteorological Institute, Helsinki, Finland

Correspondence to: Anna Nikandrova (anna.nikandrova@helsinki.fi)

Abstract. Understanding the distribution of aerosol layers is important for determining long-~~-~~range transport and aerosol radiative forcing. In this study we combine airborne in situ measurements of aerosol with data obtained by a ground-based High Spectral Resolution Lidar (HSRL) and radiosonde profiles to investigate the temporal and vertical variability of aerosol properties in the lower troposphere. The HSRL was deployed in Hyytiälä, Southern Finland, from January to September 2014 as a part of the US DO~~e~~E ARM (Atmospheric Radiation Measurement) mobile facility during the BAECC (Biogenic Aerosols – Effects on Cloud and Climate) Campaign. Two flight campaigns took place in April and August 2014 with instruments measuring the aerosol size distribution from 10 nm to 5~~10~~ µm at altitudes up to 3800 m. Two case studies from the flight campaigns, when several aerosol layers were identified, were selected for further investigation: one clear sky case, and one partly cloudy case. During the clear sky case, turbulent mixing ensured small~~low~~ temporal and spatial variability in the measured aerosol size distribution in the boundary layer whereas mixing was not as homogeneous in the boundary layer during the partly cloudy case. The elevated layers exhibited larger~~greater~~ temporal and spatial variability in aerosol size distribution, indicating a lack of mixing. New particle formation was observed in the boundary layer during the clear sky case, and nucleation mode particles were also seen in the elevated layers that were not mixing with the boundary layer. Interpreting local measurements of elevated layers in terms of long-range transport can be achieved using back trajectories from Lagrangian models, but care should be taken in selecting appropriate arrival heights, since the modelled and observed layer heights did not always coincide. We conclude that higher confidence in attributing elevated aerosol layers with their air mass origin is attained when back trajectories are combined with lidar and radiosonde profiles.

1 Introduction

Aerosols are tiny particles suspended in the atmosphere that severely affect human health (Tie et al, 2009; Apte et al., 2015; Pope et al., 2015) and climate. Most of the particles have a direct cooling effect on climate by scattering solar radiation

(McCormick and Ludwig, 1967; Sundström et al., 2015, Lacagnina et al., 2017) and indirect by changing cloud properties (Haywood and Boucher, 2000; Ten Hoeve and Augustine, 2016; Saponaro et al., 2017), yet some of the particles have a warming effect by absorbing solar radiation (Yu et al., 2006). The average lifetime of aerosol particles in the boundary layer (BL) varies from several hours to two weeks (Seinfield and Pandis, 2006) and they can be transported far from their source of origin. However, they are not distributed uniformly, with aerosol concentrations and properties varying significantly in space and time. Thus, it is challenging to implement aerosol schemes in global climate models (Myhre et al., 2013; Zhang et al., 2016; Glassmeier et al., 2017) and the impact of aerosol remains one of the largest sources of uncertainty in climate predictions (IPCC, 2013).

Most aerosol particles are emitted from the surface (Kaufman et al., 2002), or are formed from their pre-cursor gases either close to the surface or higher up in the free troposphere (e.g. Kulmala et al, 2004, 2007, 2013; Dunne et al., 2016). Turbulent mixing distributes aerosol uniformly throughout the well-mixed BL, but stable stratification elsewhere in the atmosphere usually inhibits any further mixing. Hence, layers can form once the source of turbulent mixing is removed, one example being the formation of residual layers after sunset (Stull, 2012). Here, we define elevated layers as those existing above the daytime well-mixed BL. This can include residual layers if the boundary-layer depth is supressed on subsequent days. Deep convection (Andreae et al., 2001, Wang et al., 2016) and mid-latitude cyclones (Sinclair et al., 2010) can transport aerosol vertically throughout the troposphere, and, once in the free troposphere, baroclinic systems can advect aerosol over long distances (Donnell et al., 2001). Wet deposition and evaporation to the gas phase are the main removal mechanisms for aerosol above the BL, although it is also possible for elevated aerosol layers to be mixed back into the BL after some time of being aloft.

The vertical distribution of aerosol particles is important for determining the direct and indirect aerosol radiative forcing (Haywood and Ramaswamy, 1998). Lidar measurements are able to track the evolution of aerosol layers with a high resolution in space and time (Wandinger et al., 2002; Groß et al., 2011; Burton et al., 2012; Pappalardo et al., 2014; Baars et al., 2016). Reid et al. (2017) looked at the monthly variability of backscatter profiles from a High Spectral Resolution Lidar (HSRL) located in Hunstsville, Alabama, US during summer and reported that aerosol backscatter was the highest below 1.5 km and decreasing with an increasing height rapidly until 3.5 km. They also observed occasionally different layering structures in the free troposphere, which was in general a clear region with low aerosol concentration. During the Two-Column Aerosol Project (TCAP, Berg et al., 2016), that studied~~ying~~ the atmospheric column both at the coast of North America and several hundred kilometres away in the Atlantic Ocean using second-generation HSRL-2 (Muller et al., 2014), elevated aerosol layers were observed on four out of six clear-sky research flights with contributions of up to 60 % to the total column aerosol optical depth. Fast et al. (2016) found that some of these elevated aerosol layers were likely lifted from the BL as a result of strong synoptic-scale convergence. ~~At higher latitudes, s~~Smoke events may be responsible for elevated layers with significant contributions to the total column aerosol optical depth (O'Neill et al., 2008).

An airborne HSRL-2 was used to constrain the vertical distribution of aerosol microphysical properties observed in California and Texas (Sawamura et al., 2017). Microphysical properties retrieved from HSRL-2 showed a good agreement with in situ measurements; however, ~~calculated~~ backscatter and extinction coefficients calculated from corresponding in situ measurements were consistently underestimated, which was attributed to the undersampling of coarse mode particles by in situ measurements. Combined data from diverse measurement campaigns over the Pacific show that the free troposphere was dominated by aerosols formed near cloud edges and in convective regions, as well as particles transported from continents (Clarke and Kapustin, 2002).

Detailed information on aerosol size distributions and microphysical properties can be obtained from in situ airborne measurements. However, compared to the quantity of aerosol measurements at the surface, there have been relatively few flight campaigns investigating elevated aerosol layers, especially at low aerosol load conditions (add reference from review 4). Boy et al. (2004), O'Dowd et al. (2009) and Schobesberger et al. (2013) conducted airborne measurements over a boreal forest, primarily interested in new particle formation (NPF). New particles were observed throughout the BL in all three studies, but Schobesberger et al. (2013) reported much lower particle concentrations outside the BL. This suggests that in the boreal forest large-scale NPF events are typically confined to the BL, ~~as only one event was detected in the free troposphere.~~similar to results found in other environments (Crumeyrolle et al., 2010; Berland et al., 2016).

In this study, our aim was to investigate aerosol layers in a rural environment, their origin, and how they change over time. We were particularly interested in how the aerosol size distribution varied both within and between layers. This information could be used to determine whether there was mixing within and between layers, and whether there had been any recent contact with the surface. For this purpose, a comprehensive set of ground-based remote sensing observations together with both airborne and ground-based aerosol measurements were collected during the Biogenic Aerosols – Effects on Cloud and Climate (BAECC) campaign in Hyytiälä, Finland during 2014 (Petäjä et al, 2016). We used HSRL measurements from the surface, and Scanning Mobility Particle Sizer (SMPS) and Optical Particle Sizer (OPS) measurements on board an aircraft, described in Section 2, to analyse aerosol layers in two case studies, described in Section 3. The first case represents typical clear-sky weather conditions during spring at the station with a clean air mass arriving from the north. This is an ideal case because the development of the BL and elevated aerosol layers could be monitored for several days without interruption. The second case is more complicated, with partly cloudy and unstable atmospheric conditions. Back trajectory analysis was conducted for both case studies to examine whether these analyses produced similar layer structures to those observed, and how closely the diagnosed layer altitudes corresponded with those observed by the HSRL.

2 Experimental setup

The SMEAR-II (Station for Measuring Forest Ecosystem-Atmosphere Relations - II, see Hari and Kulmala, 2005) measurement station located in Hyytiälä, southern Finland (61 51 N, 24 17 E, 181 m a.s.l.), is a rural background station with no major anthropogenic emission sources located nearby. During the BAECC campaign, the US Department of Energy Atmospheric Radiation Measurement (ARM) programme deployed the HSRL in Hyytiälä from January to September 2014 as a part of the ARM mobile facility (AMF). Vaisala RS92 radiosondes (RS) were launched 4 times a day during the campaign (nominally at 00Z, 06Z, 12Z and 18Z).

2.1. Instrumentation

High Spectral Resolution Lidar

The AMF HSRL (Shipley et al., 1983; Grund and Eloranta, 2005; She et al., 1992) is an autonomous lidar system designed to retrieve vertical profiles of the backscatter coefficient, extinction coefficient, and depolarizsation. The system uses a frequency-doubled Nd:YAG laser emitting pulses at a wavelength of 532 nm and a repetition rate of 4 kHz, together with an afocal telescope with a diameter of 40 cm acting as both transmitter and receiver. The telescope has a field of view of 45 µrad, which limits the impact of multiple scattering, and the large expansion of the outgoing beam means that the system is eye-safe, permitting the flight campaign to operate in the immediate vicinity of the instrument. Continuous profiles can be detected from around 50 m up to 30 km in altitude. The emitted laser light is circular-polarised. The detection chain utilises photon counting to record the atmospheric return in three channels: combined, molecular, and cross-polarisation, at 0.5 seconds and 7.5 m resolution. The combined channel contains backscattering from both particulates and molecules, whereas the molecular channel includes an iodine absorption filter (Eloranta and Razenkov, 2006) in the path to record molecular scattering only, and the cross-polarisation channel measures the degree of circular depolarizsation relative to the combined channel. Full details on the instrument setup are available in the ARM HSRL instrument handbook (Goldsmsith, 2016). The profile of attenuation is determined from the known profile of molecular scattering, enabling direct retrievals of extinction, backscatter, and particulate depolarisation up to an optical depth of 4. To reduce noise, the raw data was averaged to 5 s and 30 m before deriving the backscatter, extinction, and circular depolarisation profiles.

Airborne aerosol measurements

In situ airborne data in the lower atmosphere were obtained with a Cessna 172 light aircraft, modified for the research flights by replacing the backseats with a rack for the instruments (see. Schobesberger et al., 2013, and Väänänen et al., 2017). The sample air was collected from under one wing, away from the engine exhaust, and transferred inside the cabin via a stainless steel tube (inner diameter 22 mm, length 4.2 m). The inlet line was a downscaled version of one used by the University of Hawaii DC-8 (McNaughton et al., 2007), and the flow of the main inlet line was kept at 50 Ll min^{-1}.

The aerosol and gas instruments were situated in a rack inside the cabin. The total aerosol number concentration was measured with an ultrafine Condensation Particle Counter (uCPC, Model 3776, TSI Inc.), whereas a Scanning Mobility Particle Sizer (SMPS) was used to determine the particle number size distribution in the diameter range of 10-230 nm with a temporal resolution of two minutes. The SMPS comprised a short Hauke type Differential Mobility Analyser (DMA) with closed-loop sheath air, and a TSI 3010 CPC as a particle counter. SMPS data were inverted using the method introduced by Collins et al (2002). An Optical Particle Sizer (OPS, Model 3330, TSI Inc.) measured the particle number size distribution in the diameter range of 300-~~95~~000 nm with a temporal resolution of 10 s. Additionally, a relative humidity sensor (Rotronic HygroClip-S, accuracy 0.8% at 23 ºC) was installed under the inlet. All particle and gas instruments were calibrated in the laboratory prior to the campaign, with errors in CPC total concentrations and SMPS particle counts below 10 %. All aerosol data were corrected to the standard temperature and pressure (100 kPa and 273.15 K).

One intensive flight campaign took place in spring and another one in autumn, 2014. A typical measurement flight took 2-3 hours and consisted of numerous legs of about 40 km in length flown above the SMEAR II measurement station at Hyytiälä. The Cessna 172 air speed was low, around 35 m s^{-1} (130 km h^{-1}), enabling a relatively high vertical resolution (300 m for SMPS and 80 m for OPS). The maximum flight ceiling was 3800 m a.s.l. A typical flight plan consisted of a climb up to the free troposphere, and constant altitude legs at different altitudes. A typical climb or descent rate during the flights was 2.5 m s^{-1}. A GPS instrument was used to record the flight track.

2.2. Methods

We investigated aerosol size distributions in the BL and elevated atmospheric layers that were identified by utilizing HSRL backscatter and depolarization fields. A wavelet decomposition was used to determine layer boundaries, similar to the approach used in STRAT (Morille et al., 2007). Since our work is based on individual case studies, suitable coefficients for the layer-detection algorithm were decided based on a visual inspection. On a clear sky day, most of the aerosol load in the boreal forest area is concentrated in the BL. Therefore, the BL was easily distinguishable by the high peaks in backscatter coefficient as a consequence of a strong aerosol scattering. Layers classified with the HSRL were confirmed with the RS measurements, where edges of layers could be seen in ~~as areas of~~ changes of~~in~~ specific and relative humidity profiles ~~most often indicate edges of layers~~. The closest in-time RS measurements were used if the time of the Cessna flight and the RS launch time did not match. We considered in this study only layers below 3800 m, as it was the maximum altitude of the Cessna.

The SMPS and OPS measurements were combined in order to obtain a size distribution ranging from 10 nm to 5~~10~~ µm. Because the SMPS measures the dry size (particles are dried prior to entry), and OPS measures the ambient size (at an ambient relative humidity), the measured SMPS size distributions were modified to represent the growth expected at the ambient relative humidity by using a growth factor (GF) calculated for a boreal forest environment using measurements from Hyytiälä station by Laakso et al. (2004). They weighted the GF for compounds with different hygroscopicity according to their

respective fractions to obtain an optimal combined GF coefficient. The correction for GF was implemented as a function of height for the SMPS data. The ambient size distributions were then grouped by similarities in the size distribution and taking into account ~~using~~ the layer boundaries found in the HSRL~~lidar~~ data. Only data in the vicinity of Hyytiälä were used, with data obtained within 50 km of the airport excluded from any analysis.

Here, we will use the term nucleation mode for particles with diameters smaller than 25 nm, Aitken mode for particles ranging from 25 to 100 nm, accumulation mode for particles from 100 nm to 1 µm, and supermicron particles for particles from 1 to ~~10~~5 µm. All times are given in the Eastern European Summer Time (UTC+3).

To look at the spatial variability of arriving air masses in space and height, we calculated 96-hour back trajectories for every 50 m for the altitudes from 500 to 3500 m AGL using the HYSPLIT model (Stein et al., 2015). The National Center for Environmental Prediction (NCEP) Global Data Assimilation System (GDAS) dataset with one degree resolution was used for the meteorological input to the model.

3 Results and Discussion

Two case studies were selected, both with air masses coming from the north but with different atmospheric conditions. The first case study (Case I) consists of 3 sequential clear-sky days with NPF events detected at the ground level each day. The second case study (Case II) consists of a single day with low-level clouds present and no NPF taking place.

3.1. Case I: typical clear sky situation during 8 - 10 April

Figure 1a displays the HSRL backscatter coefficient from 50 m to 4000 m for Case I, with hi)igher values of backscatter cross section indicating either higher particle concentrations or larger particle sizes. The figure illustrates how the BL and other layers were developing, evolving and mixing during this period. The amount of lidar depolarization, shown in Fig. 1b, depends on the particle shape, and also clearly illustrates the evolving atmospheric structures and their boundaries. Sharp changes in the relative humidity (RH) seen in the RS profiles also agree with the layer determination obtained from the HSRL backscatter cross section and depolarization. However, not all HSRL determined layers exhibit a corresponding change in RH (for example, during 8 April at 14:00 at 2800 m).

The simplified layer structure shown in Fig. 1c was obtained from the HSRL backscatter and depolarization fields. Four layers were identified, denoted as the first, middle, upper and high layers. The first layer includes both the BL and the residual layer as it was not possible to separate them with our simple algorithm. Figure 1c demonstrates that, in April, the first layer in Hyytiälä can reach up to 1500 m during the day, and is usually shallow at night (lower than 1000 m). There were several elevated layers on 8 April, one of which disappeared during the day, with no major new layers appearing on 9 April. On 10

April, a new layer exhibiting high backscattering and low depolarisation developed at around 2500 m. Additionally, a narrow band with a high backscatter cross section (relative to surroundings) during 9 and 10 April was initially classified as a separate layer and then termed an interface zone after a closer inspection. The interface zone was a shallow zone situated at the boundary between two more substantial layers and was characterized by depolarization values different from the surroundings and large backscatter values. No corresponding thin layer was detected in the humidity profiles, whether from the radiosonde or aircraft. During these three days, six flights were made with the Cessna (one morning flight and one afternoon flight each day). Four flights were selected for analysis; these are described in more detail below and summarised in Table 1. In figure 2, for each flight, a panel comprising three plots displays 1) radiosonde profiles of RH and specific humidity mixing ratio; 2) time-height HSRL backscatter cross section with the Cessna flight altitude superimposed; and 3) mean and +/- one standard deviation of the aerosol size distribution obtained from SMPS and OPS measurements within each layer.

3.1.1. Case I: Flight descriptions

Four layers in the HSRL backscatter coefficient were recognized during the Cessna flight between 16:00 and 17:30 EEST on 8 April 2014, as shown in Fig. 2b. The RH and specific humidity mixing ratio from the RS (Fig. 2a), launched two hours before the flight at 14:22 EEST, also shows several distinct layers in the profile which correspond well with those identified by the HSRL. The profile of the specific humidity mixing ratio indicated that the BL~~this~~ layer was well mixed, whereas the corresponding values were changing through the other layers.

The size distributions displayed four distinct distribution shapes corresponding to the four layers observed by the HSRL (Fig. 2c). The BL was characterized by high aerosol concentrations of up to 6000 cm^{-3} in the Aitken mode, due to the NPF event that took place earlier in the afternoon. The lowest concentrations of Aitken mode particles were found in the first middle layer. The second middle layer had a similar size distribution shape for particles smaller than 100 nm but higher concentrations, and displayed the highest concentrations of supermicron particles, even higher than in the BL. The second middle layer also exhibited much more depolarisation than the other layers (Fig. 1b), together implying long-range transport of large non-spherical particles. Nucleation mode particle concentrations were higher than Aitken mode particle concentrations in both middle layers, whereas no particles smaller than 15 nm were detected in the upper layer. However, the upper layer had much higher concentrations of 20-40 nm particles than the other elevated layers.

The first Cessna flight on 9 April took place from 11:00 to 12:30 EEST (Fig. 2d-f). Three distinct layers were observed below 3500 m, also visible in the RS humidity profiles. The middle layer was significantly drier than both the BL and the layer above. The mean aerosol size distribution in the BL is shown separately for the ascent and descent profiles (Fig. 2f), illustrating that there was a notable increase in the nucleation mode particle concentration during the descent. The middle layer was characterized by a low Aitken mode concentration and high accumulation and supermicron mode concentrations. The upper layer displayed a similar aerosol size distribution shape to the one in the BL, but with considerably smaller concentrations.

The same three layers were seen during the second Cessna flight, which took place from 16:00 until 17:40 EEST (Fig. 2g-i). The humidity profiles were also similar to the morning flight. The impact of the NPF and subsequent growth is clearly seen in the BL aerosol size distribution (Fig. 2i), with Aitken mode concentrations reaching 5000 cm^{-3}, much higher than observed during the morning. The size distributions in the middle and upper layer were similar to the morning flight except for the nucleation mode. No particles smaller than 15 nm were detected in the upper and middle layers during the morning flight, but these were observed in the afternoon flight, providing evidence for NPF in elevated layers.

On 10 April the Cessna flew in the afternoon from 13:45 to 15:30 EEST (Fig. 2j-l). Three distinct layers are visible in the humidity profiles, but the HSRL data suggests four, subdividing the upper layer into two. In addition, the HSRL observed a very thin layer which we will discuss separately in section 3.1.5. The aerosol size distributions in each layer are similar to those in the previous day. The upper layer also exhibited higher concentrations in the supermicron mode.

3.1.2. Case I: Size distribution variability within layers

We also investigated the variability in the aerosol size distribution within each layer, which is illustrated in Fig. 2c,f,i,l with the standard deviation above and below the mean size distribution for each layer. The smallest~~least~~ variability was usually observed in the BL, indicating that this layer was well-mixed vertically and horizontally with similar aerosol concentrations at all heights. Large variability was sometimes seen in the ultrafine range in the BL, which was attributed to NPF events (Dal Maso et al., 2005, Tunved et al., 2006, Kulmala et al., 2013). NPF events took place every day during the case study period. For the morning flight on 9 April, the variability for all size ranges was small~~low~~ during the ascent but increased in the ultrafine range during the descent (Fig. 2f); the ascent and descent profiles were separated by an hour and the NPF event began after the Cessna left the BL while ascending. During the afternoon flight on the same day 4 hours later, when the NPF event had finished, the BL appeared homogeneous again with a small ~~low~~ variability for almost all sizes except for particles between 20 and 30 nm (Fig. 2i). On 10 April, the variability in the BL nucleation mode was also quite high, a result of the NPF event still ongoing (Fig. 2l).

In contrast, a larger~~higher~~ variability in the size distribution was seen for the elevated layers, where there is much less turbulent mixing, with more variation seen at almost all size ranges. The middle layer exhibited a similar variability across all three days, whereas the upper layer showed some changes from day to day, probably due to changes in the depth of the layer. On 8 April, the upper layer appeared to be less than 500 m deep, but was as much as 1900 m deep on 9 April. It is difficult to ascertain the variability in the nucleation mode size range (< 25 nm) for the elevated layers, as there may have been no particles, or too few for the instrument to obtain reliable counts.

~~Low instrument counts for the largest OPS sizes introduces sampling errors leading to an apparent large variability below concentrations of about 0.1 cm^{-3} for all the layers.~~

3.1.3. Case I: Back- trajectory analysis

Figure 3 shows the origin of the air masses arriving at SMEAR II each day for Case I, based on HYSPLIT back- trajectories. The trajectories were separated into layers based on similarities in origin and the tracks in altitude over which they were advected. During 8 April most trajectories were from the north-west after spending some time over Greenland and the North Sea. Trajectories at the lowest altitudes, associated with the BL, came more from the Arctic Ocean (two lighter green shades in Figs. 3a-b). During 9 and 10 April, BL trajectories still arrived from the Arctic Ocean, but from further east.

The middle layer (yellow colour in Fig. 3) showed the largest variation in air mass origin, with trajectories arriving from Greenland on 8 April having been at lower altitudes of around 1000 m ~~close to the surface~~ two days before their arrival, and then from the Arctic Ocean on 9 and 10 April having descended from higher altitudes of 4000 to 6000 m. The descent from higher altitudes implies drier air once it descends. This change in the middle layer was seen in the RS profiles in Fig. 1a; the relatively moist middle layer on 8 April giving way to a relatively dry layer on 9 April.

The air mass origin for the upper layer (blue colour in Fig. 3) remained the same throughout Case I, arriving via Greenland having previously been over the North Atlantic. All the trajectories had previously been ~~close to the surface~~at altitudes of 1000 m, then elevated to altitudes above 3000 m for several days before reaching the station. This layer was always dominated by Aitken mode particles (see aerosol size distributions in Fig. 2); the aerosol particles did not have the right conditions to grow larger than the Aitken mode because the upper layer was relatively dry and had probably not been in contact with the ground-based emissions of aerosol precursor compounds for at least several days. Figures 3c and 3f also indicate that the interface layer (in red) on 10 April was at the altitude where trajectories arrived from two distinct spatial origins.

Overall, the air masses separated using backward trajectories corresponded very well with the layers recognized using the HSRL. The altitudes did not match perfectly, especially with regard to the thickness of the elevated layers and the height of the BL. During 9 and 10 April, for example, the trajectory BL height was lower than the BL seen from the HSRL and, consequently, the trajectory analysis suggested a thicker middle layer. BL height diagnosed from trajectory analyses was 50-800 m lower than that observed, whereas for elevated layers, the layer boundary heights were better represented, with departures typically less than 200 m. These larger height differences for layers associated with the BL top are attributed to the difficulties that meteorological models have in representing the BL (e.g. Holtslag et al., 2013), which are then propagated through to the trajectories.

3.1.4. Case I: Evolution of the elevated layers

The evolution of the mean aerosol size distribution for the middle layer during Case I is shown in Fig. 4a. The aerosol particle concentrations remained similar across all the size ranges, except for sizes within the nucleation mode, and an increase in accumulation mode particle number concentrations was observed between 8 and 9 April. The change in accumulation mode is attributed to the change in air mass during this time. The lack of variation for most sizes indicates that there was essentially no mixing between the middle layer and the surrounding layers during this period. The large increase in nucleation mode particle concentrations for the afternoon flight of 9 April demonstrated that new particles could be formed in this layer.

In contrast, the upper layer exhibited a wide degree of variation in the aerosol size distributions across the three days of Case I (Fig. 4b). For particles smaller than 300 nm, the shape of the size distribution and concentrations changed from day to day. For particles larger than 300 nm, while the shape of the distribution remained similar, the number concentration varied across all 3 days. ~~The distribution shape remained similar for particles larger than 300 nm, whereas the concentration varied, being the highest during 10 April and the lowest during the morning flight on 9 April. In the smaller particle range, the shape of the distribution was also similar, with an exception of 10 April, possibly due to the influence of an extra layer on April 10.~~ This layer might have been mixing with air higher up in the troposphere.

3.1.5. Case I: Interface layer

We examined separately a thin 150 m boundary between the middle and upper layers during 10 April. This layer was characterized by strong scattering seen in the HSRL backscatter coefficient at around 1900 m (Fig. 2k) and it was located in the area of RH change from 5 % to 15 %. Backward trajectories showed that this layer was a section where air masses of two different origins and heights intersected. The panels of Fig. 5 demonstrate the total particle concentration measured by the CPC and uCPC during the ascent, the OPS data with a 10 s time resolution, as it was impossible to trace this interface layer only with the two minute time resolution data of the SMPS. The HSRL backscatter cross section data were averaged over the time of the Cessna ascent. Peaks on all three panels occurred at the same height of 1900 m. On the first panel, showing the measurements of the CPC and uCPC, there was a peak in the total particle concentration, whereas concentrations of particles smaller than 10 nm, measured by the uCPC, did not change. A very high peak of 33 particles cm^{-3} in comparison to the rest of the profile was seen on the total concentration of particles of 0.3 μm to ~~10~~5 μm, measured by the OPS. When the size distribution was examined, it was found that the contribution to this peak came from particles in the diameter range of 300-500 nm. This thin layer could be either a result of limited small-scale mixing between two layers, that were probably stable, or the result of large-scale transport of smoke or dust; however, we suspect that this is a response of aerosol growing rapidly as it moves from very dry air to much moister conditions, especially since the low HSRL circular depolarization values suggests that particles in this thin layer were relatively spherical ~~This thin layer could be either a result of limited small-scale mixing~~

~~between two layers, that were probably stable, or the result of large-scale transport of aged dust, especially since the low HSRL circular depolarisation values suggest more spherical particles.~~ More data and further analyses are needed to understand the processes that lead to higher values of a backscatter cross section in these interface areas.

3.2. Case II: cloudy during 22 August

Figure 6 shows HSRL backscatter coefficient and circular depolarization ratio from 50 m to 4000 m for Case II. Backscatter values were, in general, higher than for Case I even though the aerosol number concentrations were similar for both cases, attributed to the much higher relative humidity in Case II resulting in significant aerosol hygroscopic growth. Fog was present from 6:00 to 9:30, severely attenuating the signal. As the fog lifted, the lidar was able to occasionally penetrate and detect the deep residual layer above that extended to 1850 m in altitude. The residual layer showed low depolarization and high backscatter values characteristic of a humid BL, in contrast to the layers above 1850 m. The BL started to mix into the residual layer during the morning at around 1100 and continued to deepen to at least 2000 m by mid-afternoon. The cloud radar showed that ~~O~~occasional cumulus clouds were formed from 1000 m in altitude~~,~~ and were able to grow to at least 3000 m in altitude by late afternoon. Ground-based measurements from the SMEAR II station indicated that there was no NPF event at the surface during this case study.

Two flights were made with the Cessna during this day, one morning flight and one afternoon flight, and these are described in more detail below. A figure with similar panels as for Case I was generated for each flight.

3.2.1. Case II: flight description

The first Cessna flight during 22 August took place from 9:30 to 10:30. Even though the HSRL signal was often fully attenuated by fog or low cloud, the height of the growing BL and the presence of the residual layer are clear in Fig. 7a-c. Both layers were also obvious in the radiosonde profile, launched one hour before the Cessna flight commenced. The BL RH was close to 100 %, hence the fog, with a constant specific humidity mixing ratio of about 7 g kg^{-1}. Between this layer and the residual layer was an entrainment zone within which the specific humidity mixing ratio was decreasing rapidly with height. The residual layer above the entrainment zone also exhibited a relatively constant specific humidity mixing ratio of about 4.5 g kg^{-1}, from 700 m to 1850 m. Above 1850 m, the specific humidity mixing ratio decreased to about 1 g kg^{-1}; the profile indicated several additional layers, but these were difficult to distinguish in the HSRL backscatter coefficient and circular depolarisation ratio.

Together with the airborne in situ measurements, seven layers were diagnosed (Fig. 7c), classified as belonging to three main groups: first (green), middle (yellow) and upper (blue) layers. The first group comprised the BL, residual layer, and the entrainment zone. As a group, these layers displayed low concentrations of nucleation mode particles, but much higher concentrations in all other modes, relative to the layers above. The three layers in this group exhibited differences mostly in

the Aitken mode: the BL and entrainment zone exhibited a peak at different sizes in the Aitken mode, whereas the residual layer exhibited a Hoppel minimum for sizes in the 0.08-0.1 µm~~80-100 nm~~ region characteristic of cloud processing (Hoppel et al., 1990). The middle group was also separated into three layers, displaying differences in the nucleation and Aitken mode number concentrations. These layers corresponded well with the humidity structure seen in the radiosonde profile. The aerosol size distribution in the upper layer was similar to the one in the lowest layer in the middle group, except for lower concentrations below 30 nm.

The second Cessna flight on 22 August took place from 14:00 to 15:30 (Fig. 7d-f). Several cumulus clouds were present during the flight and can be seen in the HSRL backscatter coefficient (Fig. 7e). The BL had now grown to consume the residual layer from the previous day, but the radiosonde profile suggests that the BL was not as well mixed as one would expect for a classical BL – the profile of specific humidity mixing ratio was not constant and RH is not always increasing with height. ~~Two tendencies are seen in the BL: a more mixed lower part up to about 1000 m where the cloud bases were, and a less mixed upper part.~~The BL was well-mixed up to 600 m, and became progressively less well mixed above this, with convectively buoyant air parcels reaching up to 2500 m. The radiosonde thermodynamic profile suggested that deep convection to 4 km or so was possible, and did indeed occur later on in the day. Three layers were identified in the airborne data: the BL and two middle layers. The shape of the aerosol size distribution in the BL was similar to the residual layer of the earlier flight, also displaying a Hoppel minimum (0.09 µm ~~90 nm~~). The middle layers were separable with respect to Aitken mode particle concentrations, and could also be diagnosed from the radiosonde profiles. They corresponded with the middle layers seen during the descent of the morning flight. The upper layer of the morning flight was not detected during this flight, due to the limitations of the Cessna flight ceiling. Interestingly, nucleation mode particles were detected in the all layers during both flights of Case II.

3.2.2. Case II: Size distribution variability within layers

The elevated layers showed the same variability in the aerosol size distribution as was observed in Case I for particles smaller than 300 nm, but smaller~~less~~ variability in the accumulation and coarse modes. The BL exhibited larger~~more~~ variability in the aerosol size distribution than was seen for the clear sky case (Case I), even during the afternoon flight (Fig. 7f). The radiosonde profiles show that the BL was not as well-mixed as in Case I, as the specific humidity mixing ratio was not constant with height (Fig. 7d), in strong contrast to the BL profiles seen in Fig. 3. The residual layer exhibited a profile of specific humidity mixing ratio that was relatively constant (Fig. 7a), presumably a result of a well-mixed BL on the previous day, but this layer was no longer turbulent and also showed some variability in the size distribution. The BL was clearly convective, but the mixing was not homogeneous, indicated by the presence of ~~deep~~ cumulus clouds that were forming as a result of more organised updrafts.

3.2.3. Case II: Back -trajectory analysis

Figure 8 shows the origin of the air masses arriving at SMEAR II each day for Case II, based on HYSPLIT back -trajectories. As for Fig. 3, the trajectories were separated into layers based on similarities in origin and the altitude tracks over which they were advected. Similar to Case I, the air mass origins were from the North, but now travelled over the relatively warm Baltic sea before arriving at the station, where air in the BL could pick up moisture and become more humid. There was little change in altitude over the four days for the majority of the back -trajectories; however, by mid-afternoon, there were some trajectories inserted into the upper portion of the BL over Hyytiälä that had been close to the surface prior to their ascent over the Norwegian mountains between 06:00 and 18:00 EEST on 20 August (Fig. 8d; light green layer).

For this case, it would have been much harder to identify any layers based on back-trajectory analysis alone, since there was not much change in altitude over time, or in spatial origin. The set of trajectories that had been elevated from the surface (Fig. 8d; light green layer), would have been mixed into the BL by the time they reached the station.

3.2.4. Case II: Evolution of the layers

The BL aerosol size distribution measured during the afternoon flight resembled the distribution seen in the residual layer during the morning flight (Fig. 9a), with a Hoppel minimum suggesting cloud processing still visible for sizes around 0.07 µm ~~70 nm~~. The afternoon BL displayed higher concentrations of nucleation mode particles than both the residual layer and morning BL, but decreased concentrations of particles above 500 nm. This may due to dilution as the growing BL entrains air from above with lower concentrations in this size range. Both middle layers showed little change in the aerosol size distribution between the morning and afternoon flights, except for small differences in the nucleation mode for the first middle layer (Fig. 9b). This may be a result of occasional localised cloud-driven entrainment when cumulus clouds begun to extend into the first middle layer during the second flight. This was also indicated in the HSRL measurements (Fig. 6 and Fig. 7e) as the BL top was more diffuse (Fig. 7c) and quite variable even on short timescales, changing by as much as 1 km in 10 minutes. The presence of cumulus clouds suggests that the BL top was spatially heterogeneous.

4 Summary and conclusions

We present an analysis of aerosol layers over a relatively clean background measurement station based on a combined dataset comprising ground-based remote sensing observations, radiosonde profiles and airborne in situ measurements. The backscatter cross section coefficient and circular depolarisation provided by HSRL, together with the radiosonde humidity profiles, were used for diagnosing layers and their evolution, while airborne SMPS and OPS measurements provided the aerosol size distribution from 10 nm to 5~~10~~ µm within each of these layers at altitudes up to 3800 m.

Two case studies were chosen: a typical clear sky situation lasting for three consequent days, and a partly cloudy day. Several elevated aerosol layers were detected in both cases. For the clear-sky case, the highest aerosol number concentrations were observed in the BL, for all modes. The radiosonde profiles indicated a classic well-mixed profile within the BL, which was also apparent in the small ~~low~~ temporal variability in the measured aerosol size distributions. Outside the well-mixed BL, the temporal variability in the measured aerosol size distributions was usually much larger. The elevated aerosol layers showed size distributions with very similar shapes to the size distribution in the BL, but the typical number concentration in each layer differed. The back trajectories suggested that most of the elevated layers had spent some time close to the surface previously, and that, since the air masses all had similar origin, and therefore aerosol source, the difference in number concentration was presumably due to the amount of dilution experienced through entrainment in each layer during transport.

Nucleation mode particles were observed in the elevated layers. Since the aerosol concentrations in one of the elevated layers remained constant for several days with essentially no mixing observed, this suggests the potential for new particle formation occurring in the elevated layer at the same time as in the BL. In addition, a thin 'interface' layer was observed, between two distinct elevated layers, containing high concentrations of particles between 300 and 500 nm. Without chemical composition information, not available on these flights, it was not possible to determine whether this thin layer was a result of small-scale mixing between two adjacent layers, or whether these particles were the result of large-scale transport of smoke or dust~~, especially since the low HSRL circular depolarisation values suggest more spherical particles~~.

In contrast to the clear sky case, the BL for the cloudy case did not appear to be as well mixed, even though a convective BL, expected to promote mixing, was clearly present. This was evident in both the radiosonde profile, and in the larger variability exhibited in the aerosol size distributions measured in the BL, implying that the organised convective structures present were responsible for the heterogeneity seen in the BL. In the BL, the aerosol size distribution displayed a Hoppel minimum suggesting cloud processing of aerosol particles, but with variations that were presumably again due to the specific nature of the updrafts and downdrafts resulting in BL mixing that was not fully homogeneous in the upper part of the BL ~~Evidence for cloud processing of aerosol particles was also seen in the BL but the amount of processing varied, presumably again due to the specific nature of the updrafts and downdrafts resulting in BL mixing that was not homogeneous.~~ Conversely, some of the convective plumes reached sufficient altitudes in the afternoon to provide a degree of mixing in the lower elevated layer, but this mixing was not spatially homogeneous.

We computed back trajectories every 50 m in altitude from HYSPLIT to assess whether the vertical layer structure could be explained in terms of air mass origins, determine whether individual elevated layers could be identified from the back trajectories, and test how reliable the arrival heights of the back trajectories were for each layer. The results show that layers diagnosed from HSRL could be identified from back trajectories, with the aid of RS humidity profiles, although the arrival heights did not always coincide. Not all layers could be identified from the back trajectories alone. Errors in trajectories

(particularly in the vertical) arise from the difficulties that the meteorological models providing the wind fields have in accurately representing vertical motion and turbulence, the boundary layer, and other sub-grid scale features (Stohl et al., 2001, Riddle et al., 2006, Hoffmann et al., 2016). Uncertainties in the horizontal can be determined using ensemble trajectory techniques (Stohl et al., 2001) but these are less likely to capture vertical discrepancies arising from processes that the meteorological model may not capture correctly, such as the boundary layer. The conclusion is that a combination of RS, HSRL and back trajectories gives much more confidence in determining the air mass origin and vertical layer extent when interpreting local measurements in terms of long-range transport.

Acknowledgements

This work was supported by the Academy of Finland Centre of Excellence program (project no 307331). HSRL and radiosonde data were obtained from the Atmospheric Radiation Measurement (ARM) Climate Research Facility, a U.S. Department of Energy Office of Science user facility sponsored by the Office of Biological and Environmental Research. We are very grateful for the collaboration with ARM during the BAECC campaign in Hyytiälä, Finland. We also acknowledge the NOAA Air Resources Laboratory (ARL) for the provision of the HYSPLIT transport and dispersion model used in this publication.

Atmospheric Radiation Measurement (ARM) Climate Research Facility. 2014, updated hourly. High Spectral Resolution Lidar (HSRL). 2014-04-08 to 2014-08-22, ARM Mobile Facility (TMP) U. of Helsinki Research Station (SMEAR II), Hyytiala, Finland; AMF2 (M1). Compiled by B. Ermold, E. Eloranta, J. Garcia and J. Goldsmith. Atmospheric Radiation Measurement (ARM) Climate Research Facility Data Archive: Oak Ridge, Tennessee, USA. Data set accessed 2014-09-25 at http://dx.doi.org/10.5439/1025200.

Atmospheric Radiation Measurement (ARM) Climate Research Facility. 2014, updated hourly. Balloon-Borne Sounding System (SONDEWNPN). 2014-04-08 to 2014-08-22, ARM Mobile Facility (TMP) U. of Helsinki Research Station (SMEAR II), Hyytiala, Finland; AMF2 (M1). Compiled by D. Holdridge, J. Kyrouac and R. Coulter. Atmospheric Radiation Measurement (ARM) Climate Research Facility Data Archive: Oak Ridge, Tennessee, USA. Data set accessed 2014-09-25 at http://dx.doi.org/10.5439/1021460.

References

Andreae, M., Artaxo, P., Fischer, H., Freitas, S., Grégoire, J. M. Hansel, A., Hoor, P., Kormann, R., Krejci, R., and Lange, L.: Transport of biomass burning smoke to the upper troposphere by deep convection in the equatorial region, Geophys. Res. Lett., 28, 951–954, 2001.

Apte, J. S., Marshall, J. D., Cohen, A. J., & Brauer, M.: Addressing Global Mortality from Ambient PM2. 5. Environ. Sci. Technol, 49(13), 8057, 2015.

Baars, H., Kanitz, T., Engelmann, R., Althausen, D., Heese, B., Komppula, M., Preißler, J., Tesche, M., Ansmann, A., Wandinger, U., Lim, J.-H., Ahn, J. Y., Stachlewska, I. S., Amiridis, V., Marinou, E., Seifert, P., Hofer, J., Skupin, A., Schneider, F., Bohlmann, S., Foth, A., Bley, S., Pfüller, A., Giannakaki, E., Lihavainen, H., Viisanen, Y., Hooda, R. K., Pereira, S. N., Bortoli, D., Wagner, F., Mattis, I., Janicka, L., Markowicz, K. M., Achtert, P., Artaxo, P., Pauliquevis, T., Souza, R. A. F., Sharma, V. P., van Zyl, P. G., Beukes, J. P., Sun, J., Rohwer, E. G., Deng, R., Mamouri, R.-E., and Zamorano, F.: An overview of the first decade of PollyNET: an emerging network of automated Raman-polarization lidars for continuous aerosol profiling, Atmos. Chem. Phys., 16, 5111-5137, doi:10.5194/acp-16-5111-2016, 2016.

Berg, L.K., Fast, J.D., Barnard, J.C., Burton, S.P., Cairns, B., Chand, D., Comstock, J.M., Dunagan, S., Ferrare, R.A., Flynn, C.J. and Hair, J.W.: The Two-Column Aerosol Project: Phase I—Overview and impact of elevated aerosol layers on aerosol optical depth. J. Geophys Res. Atmos., 121(1), 336-361, doi:10.1002/2015JD023848, 2016.

Berland, K., Rose, C., Pey, J., Culot, A., Freney, E., Kalivitis, N., Beckmann, M et al.: Spatial extent of new particle formation events over the Mediterranean Basin from multiple ground-based and airborne measurements. Atmos. Chem. Phys., *17*(15), 9567, 2017.

Boy, M., Petäjä, T., Maso, M.D., Rannik, Ü., Rinne, J., Aalto, P., Laaksonen, A., Vaattovaara, P., Joutsensaari, J., Hoffmann, T. and Warnke, J.: Overview of the field measurement campaign in Hyytiälä, August 2001 in the framework of the EU project OSOA, Atmos. Chem. Phys., 4(3), 657-678, doi:10.5194/acp-4-657-2004, 2004.

Burton, S. P., Ferrare, R. A., Hostetler, C. A., Hair, J. W., Rogers, R. R., Obland, M. D., Butler, C. F., Cook, A. L., Harper, D. B. and Froyd, K. D.: Aerosol classification using airborne High Spectral Resolution Lidar measurements-methodology and examples. Atmospheric Measurement Techniques, 5, 73, doi:10.5194/amt-5-73-2012, 2012.

Clarke, A. D., and Kapustin, V.N.*:* A Pacific aerosol survey. Part 1: A decade of data on particle production, transport, evolution, and mixing in the troposphere, J. Atmos. Sci., 59, 363–382, 2002.

Collins, D. R., Flagan, R. C. and Seinfeld, J. H.: Improved inversion of scanning DMA data, Aerosol. Sci. Technol., 36, 1-9, 2002.

Crumeyrolle, S., Manninen, H. E., Sellegri, K., Roberts, G., Gomes, L., Kulmala, M., Weigel, R.,, P. Laj, P. and Schwarzenboeck, A.: New particle formation events measured on board the ATR-42 aircraft during the EUCAARI campaign. Atmos. Chem. Phys., *10*(14), 6721-6735, 2010.

Dal Maso, M., Kulmala, M., Riipinen, I., Wagner, R., Hussein, T., Aalto, P. P., and Lehtinen, K. E.: Formation and growth of fresh atmospheric aerosols: eight years of aerosol size distribution data from SMEAR II, Hyytiala, Finland. Boreal Environment Research, 10(5), 323, 2005.

Donnell, E. A., Fish, D. J., Dicks, E. M. and Thorpe, A. J.: Mechanisms for pollutant transport between the boundary layer and the free troposphere, J. Geophys. Res., 106(D8), 7847–7856, doi:10.1029/2000JD900730, 2001.

Dunne, E. M., Gordon, H., Kürten, A., Almeida, J., Duplissy, J., Williamson, C., Barmet, P. et al.: Global particle formation from CERN CLOUD measurements, Science, doi:10.1126/science.aaf2649, 2016.

Eloranta, E.: High Spectral Resolution Lidar. In Lidar (pp. 143-163), Springer-Verlag, New York, 2005.

Eloranta, E. W. and Razenkov, I. A.: Frequency locking to the center of a 532 nm iodine absorption line by using stimulated Brillouin scattering from a single-mode fiber, Optics Letters, 31, 234-237, 2006.

Fast, J.D., Berg, L.K., Zhang, K., Easter, R.C., Ferrare, R.A., Hair, J.W., Hostetler, C.A., Liu, Y., Ortega, I., Sedlacek, A. and Shilling, J.E.: Model representations of aerosol layers transported from North America over the Atlantic Ocean during the Two-Column Aerosol Project, J. Geophys. Res. Atmos., 121(16), 9814-9848, doi:10.1002/2016JD025248, 2016.

Glassmeier, F., Possner, A., Vogel, B., Vogel, H., and Lohmann, U.: A comparison of two chemistry and aerosol schemes on the regional scale and the resulting impact on radiative properties and liquid- and ice-phase aerosol–cloud interactions, Atmos. Chem. Phys., 17, 8651-8680, https://doi.org/10.5194/acp-17-8651-2017, 2017.

Goldsmith, J.: High Spectral Resolution Lidar (HSRL) Instrument Handbook. No. DOE/SC-ARM-TR-157. DOE Office of Science Atmospheric Radiation Measurement (ARM) Program (United States), 2016.

Groß, S., Tesche, M., Freudenthaler, V., Toledano, C., Wiegner, M., Ansmann, A., Althausen, D. and Seefeldner, M.: Characterization of Saharan dust, marine aerosols and mixtures of biomass-burning aerosols and dust by means of multi-wavelength depolarization and Raman lidar measurements during SAMUM 2. Tellus B, 63: 706–724. doi:10.1111/j.1600-0889.2011.00556.x, 2011.

Grund, C.J. and Eloranta, E.W.: University of Wisconsin high spectral resolution lidar. Optical Engineering, 30(1), 6-12, 1991

Hari, P. and Kulmala, M.: Station for Measuring Ecosystem-Atmosphere relations (SMEAR II), Boreal Env. Res., 10, 315-322, 2005.

Haywood, J., and Boucher, O.: Estimates of the direct and indirect radiative forcing due to tropospheric aerosols: A review, Rev. Geophys., 38(4), 513–543, doi:10.1029/1999RG000078, 2000.

Haywood, J.M. and Ramaswamy, V.: Global sensitivity studies of the direct radiative forcing due to anthropogenic sulfate and black carbon aerosols. J. Geophys. Res. Atmos., 103(D6), 6043-6058, doi:10.1029/97JD03426, 1998.

Hoffmann, L., Rößler, T., Griessbach, S., Heng, Y. and Stein, O.: Lagrangian transport simulations of volcanic sulfur dioxide emissions: Impact of meteorological data products, J. Geophys. Res.: Atmos., **121**, 9, (4651-4673), 2016.

Holtslag, A.A., Svensson, G., Baas, P., Basu, S., Beare, B., Beljaars, A.C., Bosveld, F.C., Cuxart, J., Lindvall, J., Steeneveld, G.J., Tjernström, M., and Van De Wiel, B.J.: Stable Atmospheric Boundary Layers and Diurnal Cycles: Challenges for Weather and Climate Models. Bull. Amer. Meteor. Soc., 94, 1691–1706, https://doi.org/10.1175/BAMS-D-11-00187.1, 2013.

Intergovernmental Panel on Climate Change [Stocker, T.F., D. Qin, G. K. Plattner, M. Tignor, S.K. Allen, J. Boschung, A. Nauels, Y. Xia, V. Bex and P.M. Midgley (eds.)]. Cambridge University Press, Cambridge, United Kingdom and New York, NY, USA, 2013.

Kaufman, Y., Tanré., D and Boucher, O.: A satellite view of aerosols in the climate system, Nature 419, 215-223, doi:10.1038/nature01091, 2002.

Kulmala, M., Vehkamäki, H., Petäjä, T., Dal Maso, M., Lauri, A., Kerminen, V., Birmili, W., and McMurry, P.: Formation and growth rates of ultrafine atmospheric particles: a review of observations, J. Aerosol Sci., 35, 143–176, 2004.

Kulmala, M., Riipinen, I., Sipilä, M., Manninen, H., Petäjä, Junninen, H., Dal Maso, M., Mordas, G., Mirme, A., Vana, M., Hirsikko, A., Laakso, L., Harrison, R., Hanson, I., Leung, C., Lehtinen, K., and Kerminen, V.-M.: Toward direct measurement of atmospheric nucleation, Science, 318, 89–92, 2007.

Kulmala, M., Kontkanen, J., Junninen, H., Lehtipalo, K., Manninen, H. E., Nieminen, T., Worsnop, D.R et al.: Direct observations of atmospheric aerosol nucleation. Science, 339(6122), 943-946, 2013.

Laakso, L., Petäjä, T., Lehtinen, K.E.J., Kulmala, M., Paatero, J., Horrak, U., Tammet, H. and Joutsensaari, J.: Ion production rate in a boreal forest based on ion, particle and radiation measurements. Atmos. Chem. Phys., 4, 1933-1943, doi:10.5194/acp-4-1933-2004, 2004.

Lacagnina, C., Hasekamp, O. P. and Torres, O.: Direct radiative effect of aerosols based on PARASOL and OMI satellite observations, J. Geophys. Res. Atmos., 122, 2366–2388, doi: 10.1002/2016JD025706, 2017.

McCormick, R.A. and Ludwig, J. H.: Climate modification by atmospheric aerosols, Science, 156(3780), 1358-1359, 1967.

McNaughton, C. S., Clarke, A. D., Howell, S. G., Pinkerton, M., Anderson, B., Thornhill, L., Hudgins, C., Winstead, E., Dibb, J. E. and Scheuer, E.: Results from the DC-8 Inlet Characterization Experiment (DICE): Airborne versus surface sampling of mineral dust and sea salt aerosols, Aerosol science and technology, 41, 136-159, 2007.

Morille, Y., Haeffelin, M., Drobinski, P. and Pelon, J.: STRAT: An automated algorithm to retrieve the vertical structure of the atmosphere from single-channel lidar data. J. Atmos. Ocean. Tech., 24(5), pp.761-775, 2007.

Myhre, G., Samset, B.H., Schulz, M., Balkanski, Y., Bauer, S., Berntsen, T.K., Bian, H., Bellouin, N., Chin, M., Diehl, T. and Easter, R.C.: Radiative forcing of the direct aerosol effect from AeroCom Phase II simulations, Atmos. Chem. Phys., 13, 1853–1877, doi:10.5194/acp-13-1853-2013, 2013.

Müller, D., Hostetler, C. A., Ferrare, R. A., Burton, S. P., Chemyakin, E., Kolgotin, A. et al: Airborne multiwavelength high spectral resolution lidar (HSRL-2) observations during TCAP 2012: vertical profiles of optical and microphysical properties of a smoke/urban haze plume over the northeastern coast of the US. Atmos. Meas. Tech., 7(10), 3487-3496, 2014.

O'Dowd, C., Yoon, Y., Junkermann, W., Aalto, P., Kulmala, M., Lihavainen, H. and Viisanen, Y.: Airborne measurements of nucleation mode particles II: boreal forest nucleation events, Atmos. Chem. Phys., 9, 937-944, doi:10.5194/acp-9-937-2009, 2009.

O'Neill, N. T., Pancrati, O., Baibakov, K., Eloranta, E., Batchelor, R. L., Freemantle, J., McArthur, L. J. B., Strong, K. and Lindenmaier, R.: Occurrence of weak, sub-micron, tropospheric aerosol events at high Arctic latitudes, Geophys. Res. Lett., 35, L14814, doi:10.1029/2008GL033733, 2008.

Pappalardo, G., Amodeo, A., Apituley, A., Comeron, A., Freudenthaler, V., Linné, H., Ansmann, A., Bösenberg, J., D'Amico, G., Mattis, I., Mona, L., Wandinger, U., Amiridis, V., Alados-Arboledas, L., Nicolae, D., and Wiegner, M.: EARLINET: towards an advanced sustainable European aerosol lidar network, Atmos. Meas. Tech., 7, 2389-2409, doi:10.5194/amt-7-2389-2014, 2014.

Petäjä, T., O'Connor, E. J., Moisseev, D., Sinclair, V. A., Manninen, A. J., Väänänen, von Lerber A, Thornton JA, Nicoll K, Petersen W, Chandrasekar, V. et al: BAECC: A field campaign to elucidate the impact of biogenic aerosols on clouds and climate. Bulletin of the American Meteorological Society, 97(10), 1909-1928, 2016

Pope III, C. A., Cropper, M., Coggins, J., & Cohen, A.: Health benefits of air pollution abatement policy: role of the shape of the concentration–response function. Journal of the Air & Waste Management Association, 65(5), 516-522, 2015.

Reid, J.S., Kuehn, R.E., Holz, R.E., Eloranta, E.W., Kaku, K.C., Kuang, S., Newchurch, M.J., Thompson, A.M., Trepte, C.R., Zhang, J. and Atwood, S.A., Hand, J.L., Holben, B.N., Minnis, P. and Posselt, D.J.: Ground-based High Spectral Resolution Lidar observation of aerosol vertical distribution in the summertime Southeast United States, J.~~ournal of~~ Geophys.~~ical~~ Res.~~earch~~: Atmospheres, 122(5), 2970-3004, doi:10.1002/2016JD025798, 2017.

Riddle, E. E., Voss, P. B., Stohl, A., Holcomb, D., Maczka, D., Washburn, K., and Talbot, R. W.: Trajectory model validation using newly developed altitude-controlled balloons during the International Consortium for Atmospheric Research on Transport and Transformations 2004 campaign, J. Geophys.. Res., 111, D23S57, doi:10.1029/2006JD007456, 2006.

Saponaro, G., Kolmonen, P., Sogacheva, L., Rodriguez, E., Virtanen, T., and de Leeuw, G.: Estimates of the aerosol indirect effect over the Baltic Sea region derived from 12 years of MODIS observations, Atmos. Chem. Phys., 17, 3133-3143, https://doi.org/10.5194/acp-17-3133-2017, 2017.

Sawamura, P., Moore, R.H., Burton, S.P., Chemyakin, E., Müller, D., Kolgotin, A., Ferrare, R.A., Hostetler, C.A., Ziemba, L.D., Beyersdorf, A.J. and Anderson, B.E.: HSRL-2 aerosol optical measurements and microphysical retrievals vs. airborne in situ measurements during DISCOVER-AQ 2013: an intercomparison study. Atmos Chem Phys Discuss., 2016.

Schobesberger, S., Väänänen, R., Leino, K., Virkkula, A., Backman, J., Pohja, T., Siivola, E., Franchin, A., Mikkilä, J. and Paramonov, M.: Airborne measurements over the boreal forest of southern Finland during new particle formation events in 2009 and 2010, Boreal Environ. Res., 18, 145-163, 2013.

Seinfeld, J. H. and Pandis, S. N.: Atmospheric chemistry and physics, John Wiley & Sons, Inc., 2nd edn., 2006.

She, C.Y., Alvarez, R.J., Caldwell, L.M. and Krueger, D.A.: High-spectral-resolution Rayleigh–Mie lidar measurement of aerosol and atmospheric profiles, Opt. Lett., 17(7), 541-543, doi:10.1364/OL.17.000541, 1992.

Shipley, S.T., Tracy, D.H., Eloranta, E.W., Trauger, J.T., Sroga, J.T., Roesler, F.L. and Weinman, J.A.: High spectral resolution lidar to measure optical scattering properties of atmospheric aerosols. 1: Theory and instrumentation, Appl. Opt., 22, 3716-3724, doi: 10.1364/AO.22.003716, 1983.

Sinclair, V. A., Gray, S. L. and Belcher, S. E.: Controls on boundary layer ventilation: Boundary layer processes and large-scale dynamics, J. Geophys. Res., 115, D11107, doi:10.1029/2009JD012169, 2010.

Stein, A.F., Draxler, R.R, Rolph, G.D., Stunder, B.J.B., Cohen, M.D., and Ngan, F.: NOAA's HYSPLIT atmospheric transport and dispersion modeling system, Bull. Amer. Meteor. Soc., 96, 2059-2077, http://dx.doi.org/10.1175/BAMS-D-14-00110, 2015.

Stohl, A., L. Haimberger, M. P. Scheele, and H. Wernli: An intercomparison of results from three trajectory models. Meteorological Applications 8, no. 2: 127-135, 2001

Stull, R. B.: An introduction to boundary layer meteorology. Springer Science & Business Media, 2012.

Sundström, A.-M., Arola, A., Kolmonen, P., Xue, Y., de Leeuw, G., and Kulmala, M.: On the use of a satellite remote-sensing-based approach for determining aerosol direct radiative effect over land: a case study over China, Atmos. Chem. Phys., 15, 505-518, https://doi.org/10.5194/acp-15-505-2015, 2015.

Ten Hoeve, J. E., and Augustine, J.A.: Aerosol effects on cloud cover as evidenced by ground-based and space-based observations at five rural sites in the United States, Geophys. Res. Lett., 43, 793–801, doi:10.1002/2015GL066873, 2016

Tie, X., Wu, D. and Brasseur, G.: Lung cancer mortality and exposure to atmospheric aerosol particles in Guangzhou, China, Atmospheric Environment, 43(14), 2375-2377, doi: 10.1016/j.atmosenv.2009.01.036, 2009.

Tunved, P., Hansson, H. C., Kerminen, V. M., Ström, J., Dal Maso, M., Lihavainen, H., Y. Viisanen, Y., Aalto, P.P., Komppula, M. and Kulmala, M.: High natural aerosol loading over boreal forests. Science, 312(5771), 261-263, 2006.

Väänänen, R., Krejci, R., Manninen, H.E., Manninen, A., Lampilahti, J., Mazon, S.B., Nieminen, T., Yli-Juuti, T., Kontkanen, J., Asmi, A. and Aalto, P.P., Vertical and horizontal variation of aerosol number size distribution in the boreal environment, Atmos. Chem. Phys. Discus., doi:10.5194/acp-2016-556, 2016.

Wandinger, U., Müller, D., Böckmann, C., Althausen, D., Matthias, V., Bösenberg, J., Weiß, V., Fiebig, M., Wendisch, M., Stohl, A. and Ansmann, A.: Optical and microphysical characterization of biomass-burning and industrial-pollution aerosols from-multiwavelength lidar and aircraft measurements, J. Geophys. Res. Atmos., 107(D21), doi:10.1029/2000JD000202, 2002.

Wang, J., Krejci, R., Giangrande, S., Kuang, C., Barbosa, H. M., Brito, J. et al: Amazon boundary layer aerosol concentration sustained by vertical transport during rainfall. Nature, 539(7629), 416, 2016.

Yu, H., Kaufman, Y.J., Chin, M., Feingold, G., Remer, L.A., Anderson, T.L., Balkanski, Y., Bellouin, N., Boucher, O., Christopher, S. and DeCola, P.: A review of measurement-based assessments of the aerosol direct radiative effect and forcing. Atmos. Chem. Phys., 6(3), 613-666, doi:10.5194/acp-6-613-2006, 2006.

Zhang, S., Wang, M., Ghan, S. J., Ding, A., Wang, H., Zhang, K., Neubauer, D., Lohmann, U., Ferrachat, S., Takeamura, T., Gettelman, A., Morrison, H., Lee, Y., Shindell, D. T., Partridge, D. G., Stier, P., Kipling, Z., and Fu, C.: On the characteristics of aerosol indirect effect based on dynamic regimes in global climate models, Atmos. Chem. Phys., 16, 2765-2783, https://doi.org/10.5194/acp-16-2765-2016, 2016.

Table 1. Case study I: flight times, diagnosed layer parameters (Boundary, Middle and Upper layers height and depth, in m) and new particle formation (NPF) start time

Date	Time EEST	BL height	MidL height	MidL depth	UppL height	UppL depth	NPF start time in Hyytiälä
8 April	16:00-17:30	1600	1600-2400 2400-3100	800 700	3100-3350	250	10:00
9 April 1	11:00-12:30	1000/1200	1000-1500	500	1500-3400	1900	11:30
9 April 2	16:00-17:40	1400	1400-1800	400	1800-3400	1600	11:30
10 April	13:45-15:30	1200	1200-2000	800	2000-2800	800	09:30

Figures

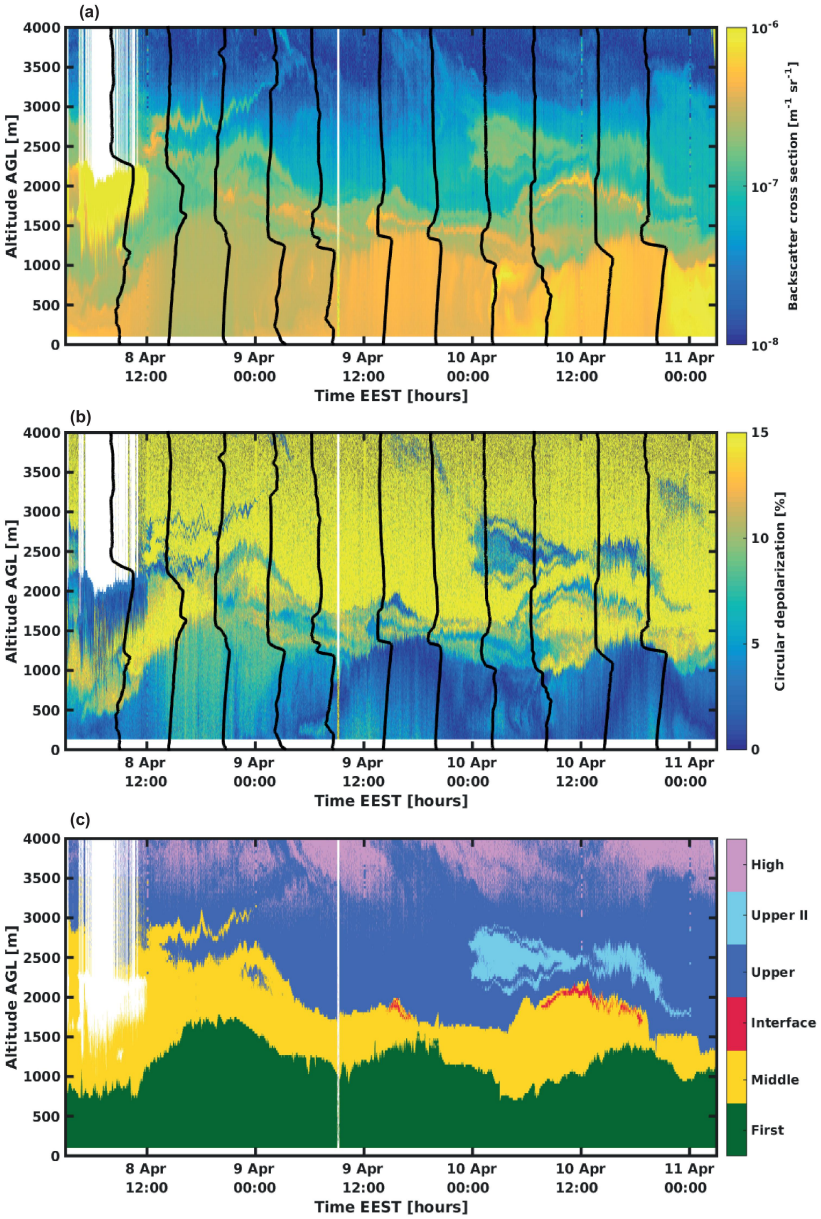

Figure 1: Case I: a) HSRL backscatter coefficient and b) HSRL circular depolarization over Hyytiälä, Finland during 8-10 April 2014, with 6-hourly radiosonde relative humidity profiles superimposed in black. Larger values of the backscatter cross section indicate higher aerosol number concentration or larger particles; larger depolarisation values suggest less spherical particles. c) Layers diagnosed from gradients in backscatter or depolarization, with the First layer (green) comprising both boundary layer and residual layer. White pixels indicate no valid measurement due to the presence of cloud and subsequent attenuation (before midday on 12 April), or due to calibration period (around 10 EEST on 9 April).

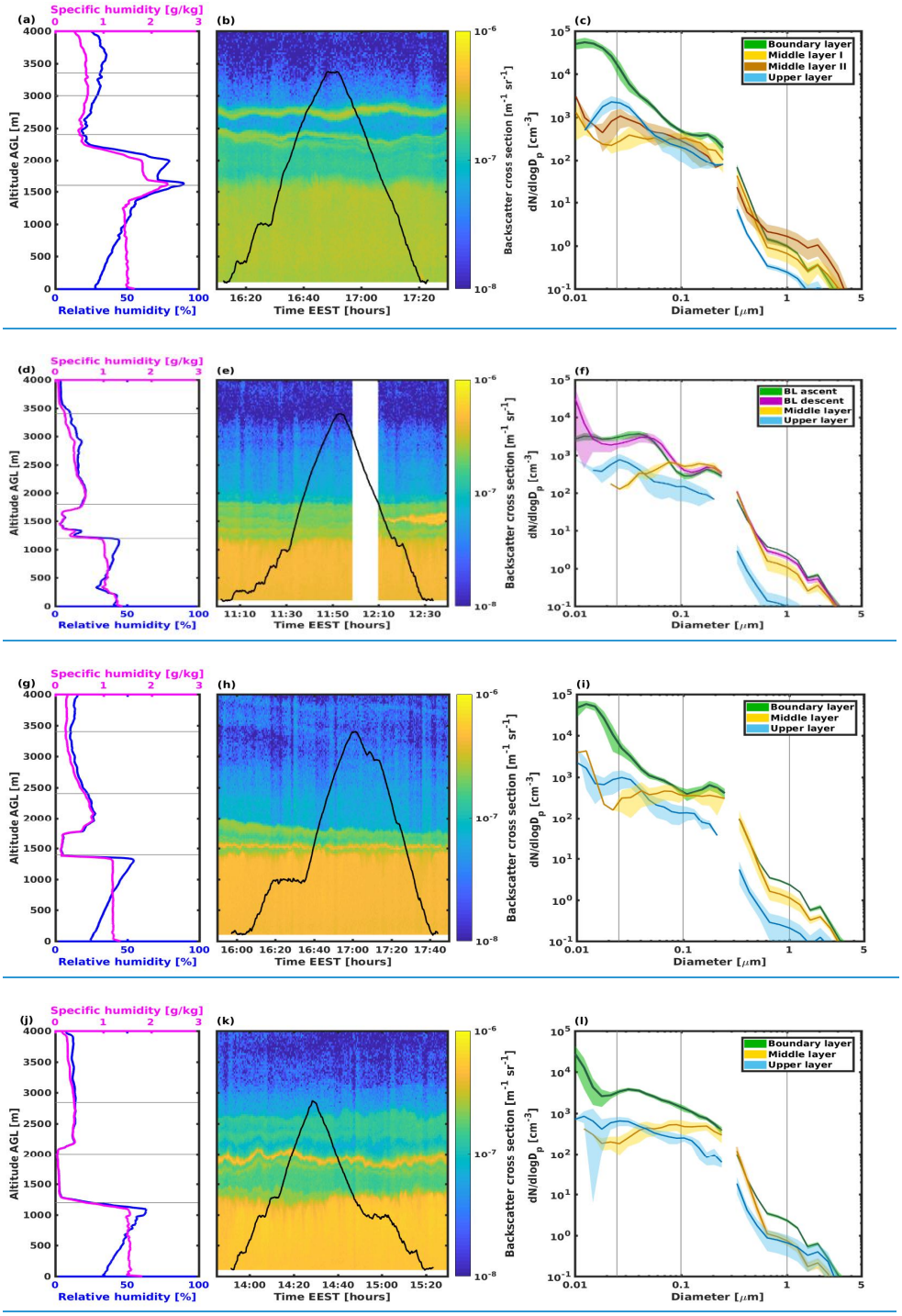

Figure 2: Four panels for each flight during Case I: a-c) 8 April, d-f) morning flight on 9 April, g-i) afternoon flight on 9 April, j-l) 10 April. Left panels show relative and specific humidity profiles measured by the radiosonde launched closest in time to the flight. Centre panels display HSRL backscatter coefficient, with Cessna flight altitude superimposed in black. Right panels present layer-

averaged aerosol size distributions from combined SMPS and OPS measurements for diagnosed layers. Mean and one standard deviation are shown for each layer. Grey lines show limits of the aerosol modes: nucleation, Aitken, accumulation and coarse.

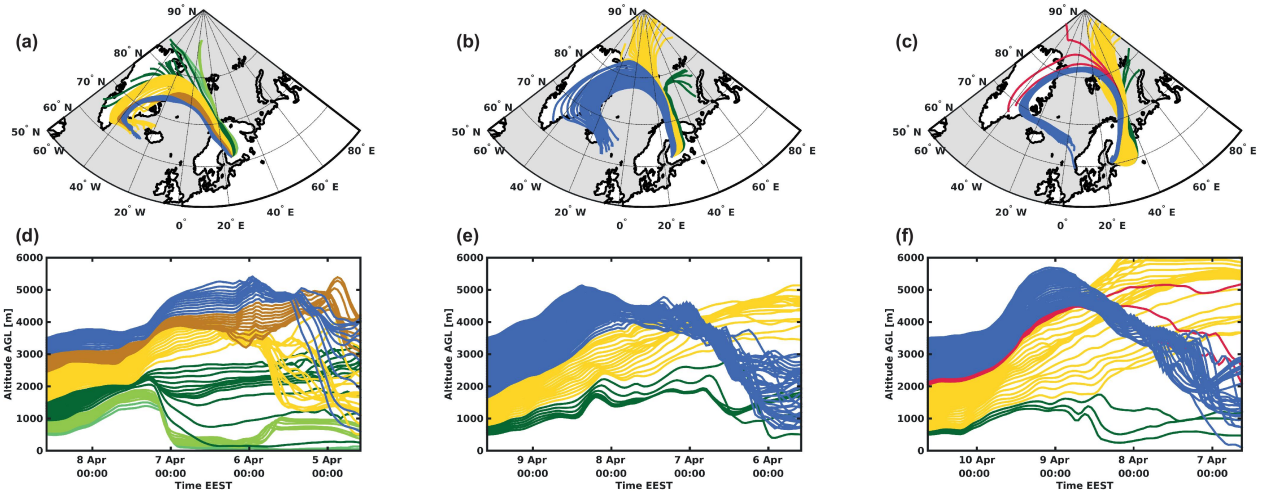

Figure 3: HYSPLIT 96-hour backward trajectories arriving at Hyytiälä calculated every 50 m in altitude from 500 m to 3500 m. Panels a-c show spatial coverage and panels d-f display the trajectory altitude over time. Trajectories with similar origin/altitude properties are combined into layers with the same colours as the layers identified with HSRL in Fig. 1c. Panels a), d) show trajectories arriving on 8 April at 17:00, panels b), e) on 9 April at 17:00 and panels c), f) on 10 April at 14.00.

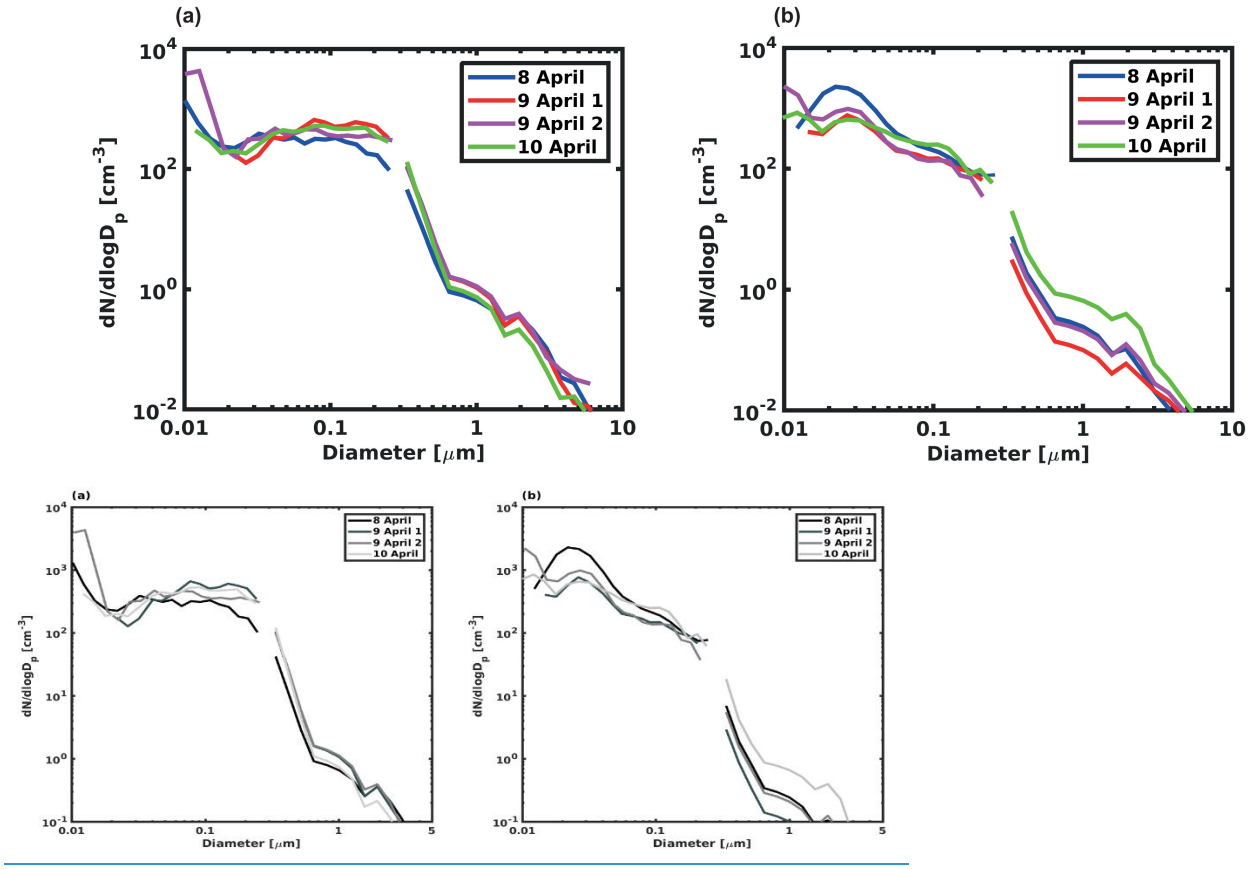

Figure 4: Evolution of the mean aerosol size distribution in Case study I for a) middle and b) upper layers. Minimal change in the size distribution during three consequent days implies that the middle layer did not mix with surrounding air. Upper layer does show changes over time, suggesting some entrainment.

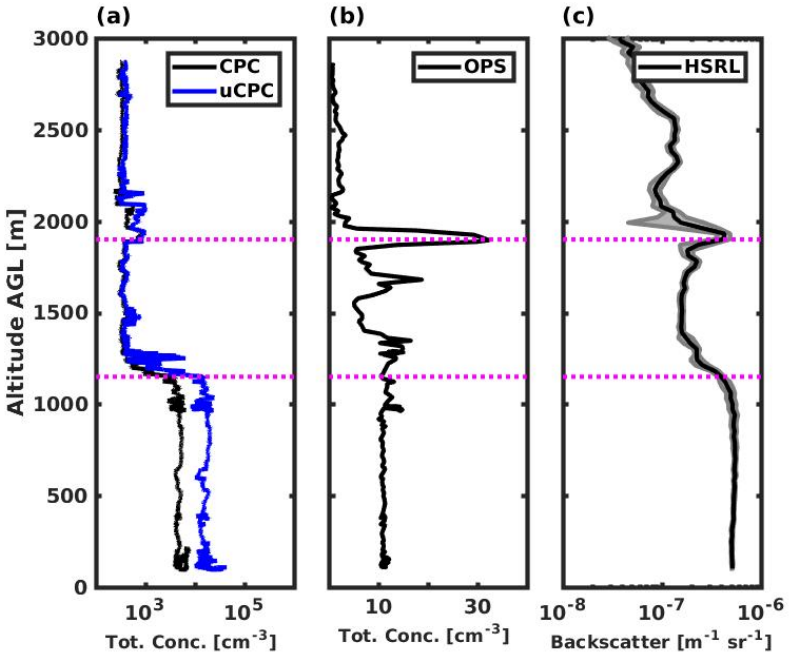

Figure 5: Vertical profiles of a) total particle concentration measured by uCPC and CPC, b) total particle concentration measured by OPS, c) HSRL backscatter coefficient averaged over the time taken for the Cessna ascent, over Hyytiälä, Finland, on 10 April 2014. All panels show a presence of a thin layer at 1900 m (dashed magenta line) with OPS indicating enhanced contribution of larger (0.3 -5~~10~~ µm) particles.

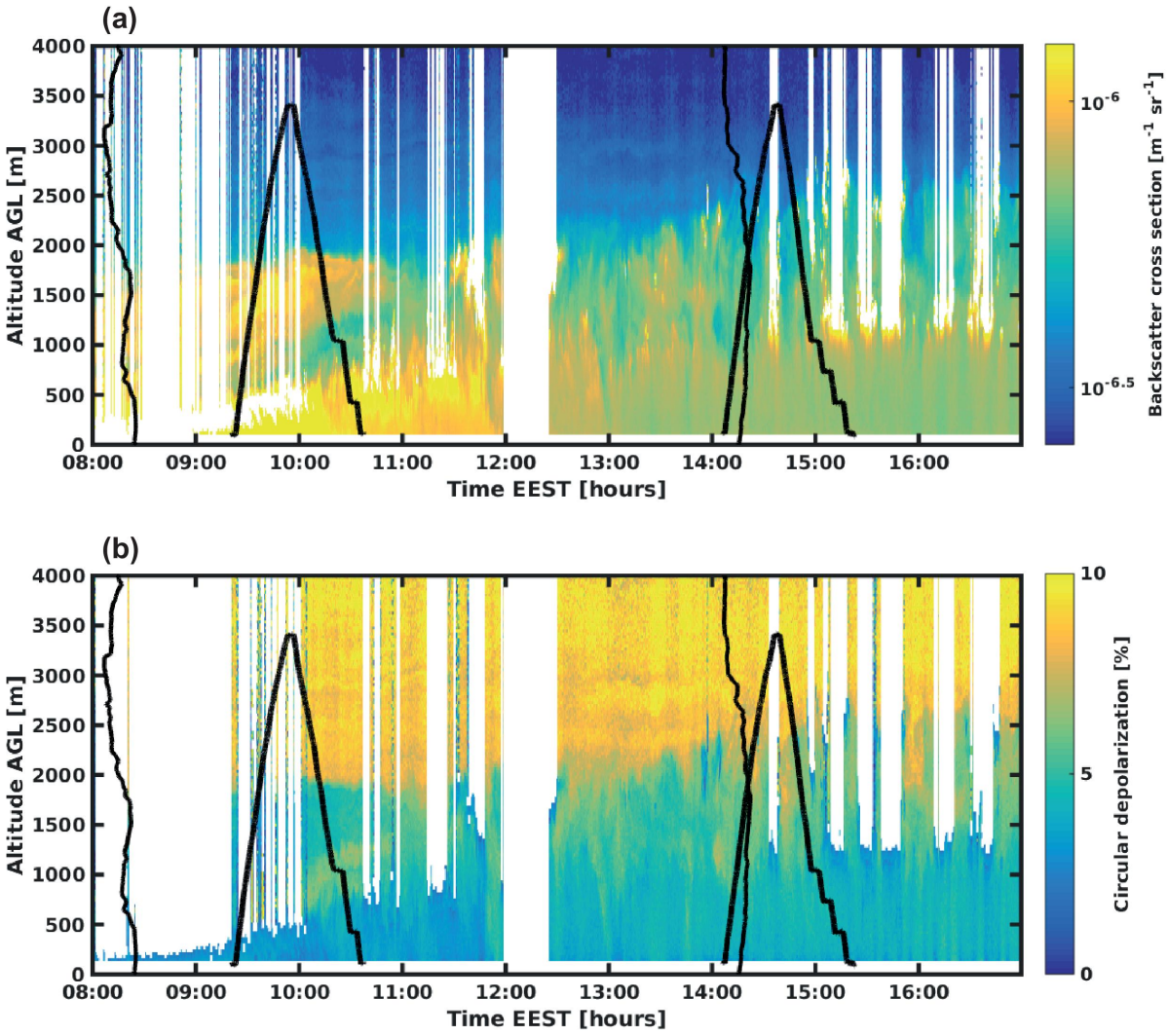

Figure 6: Case II: a) HSRL backscatter coefficient and b) HSRL circular depolarization over Hyytiälä, Finland during 22 August 2014, with 6-hourly radiosonde relative humidity profiles, and the two Cessna flight altitude tracks superimposed in black. White pixels indicate no valid measurement due to the presence of cloud and subsequent attenuation above or maintenance periods.

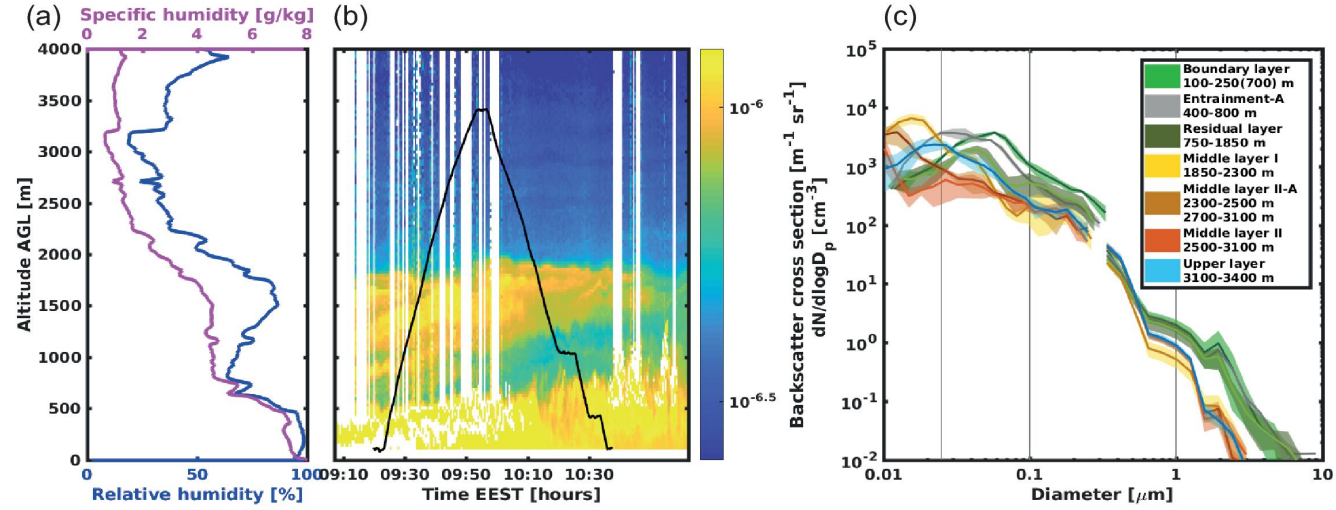
(a)
Specific humidity [g/kg]
0 2 4 6 8
Altitude AGL [m]
0 500 1000 1500 2000 2500 3000 3500 4000
0 50 100
Relative humidity [%]
(b)
09:10 09:30 09:50 10:10 10:30
Time EEST [hours]
10^{-6}
$10^{-6.5}$
(c)
Backscatter cross section [m^{-1} sr^{-1}]
$dN/dlogD_p$ [cm^{-3}]
10^{5} 10^{4} 10^{3} 10^{2} 10^{1} 10^{0} 10^{-1} 10^{-2}
0.01 0.1 1 10
Diameter [μm]
Boundary layer
100-250(700) m
Entrainment-A
400-800 m
Residual layer
750-1850 m
Middle layer I
1850-2300 m
Middle layer II-A
2300-2500 m
2700-3100 m
Middle layer II
2500-3100 m
Upper layer
3100-3400 m

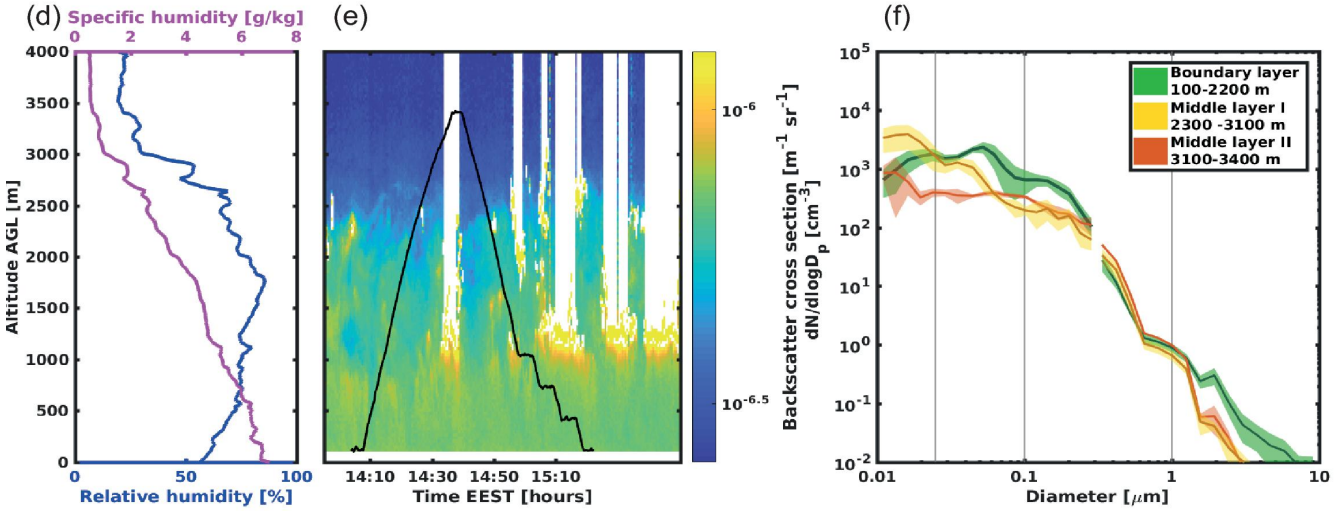
(d)
Specific humidity [g/kg]
0 2 4 6 8
Altitude AGL [m]
0 500 1000 1500 2000 2500 3000 3500 4000
0 50 100
Relative humidity [%]
(e)
14:10 14:30 14:50 15:10
Time EEST [hours]
10^{-6}
$10^{-6.5}$
(f)
Backscatter cross section [m^{-1} sr^{-1}]
$dN/dlogD_p$ [cm^{-3}]
10^{5} 10^{4} 10^{3} 10^{2} 10^{1} 10^{0} 10^{-1} 10^{-2}
0.01 0.1 1 10
Diameter [μm]
Boundary layer
100-2200 m
Middle layer I
2300 -3100 m
Middle layer II
3100-3400 m

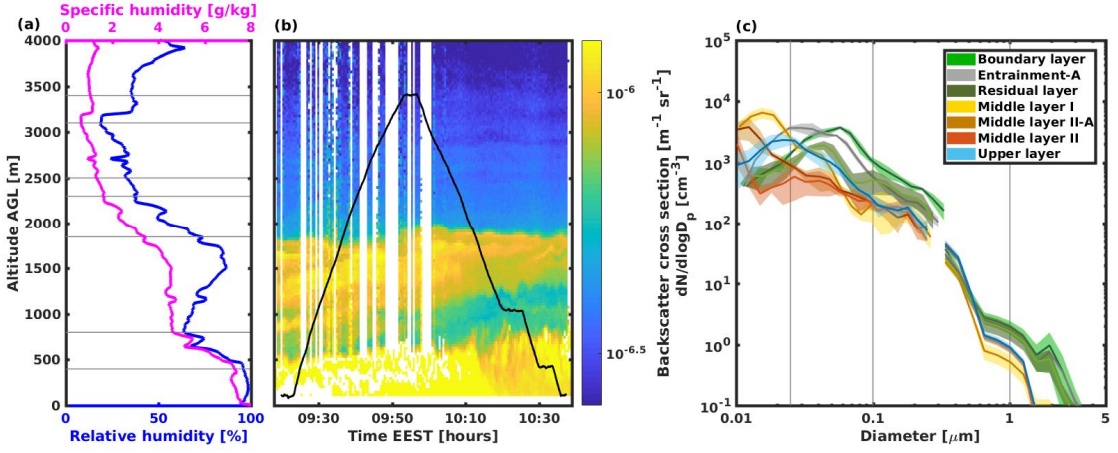
(a)
Specific humidity [g/kg]
0 2 4 6 8
Altitude AGL [m]
0 500 1000 1500 2000 2500 3000 3500 4000
0 50 100
Relative humidity [%]
(b)
09:30 09:50 10:10 10:30
Time EEST [hours]
10^{-6}
$10^{-6.5}$
(c)
Backscatter cross section [m^{-1} sr^{-1}]
$dN/dlogD_p$ [cm^{-3}]
10^{5} 10^{4} 10^{3} 10^{2} 10^{1} 10^{0} 10^{-1}
0.01 0.1 1 5
Diameter [μm]
Boundary layer
Entrainment-A
Residual layer
Middle layer I
Middle layer II-A
Middle layer II
Upper layer

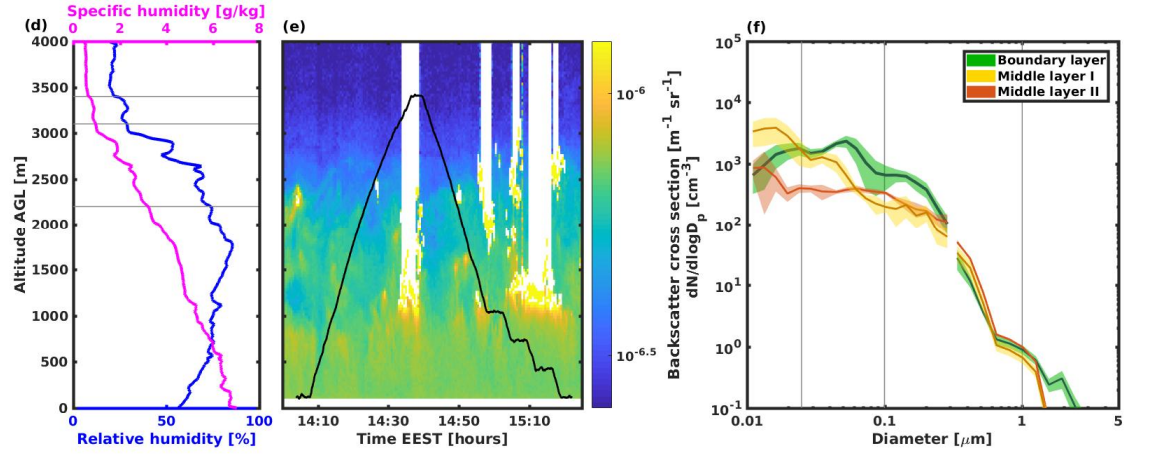

Figure 7: Same as Fig. 2 except for Case II with a-c) morning flight d-f) afternoon flight.

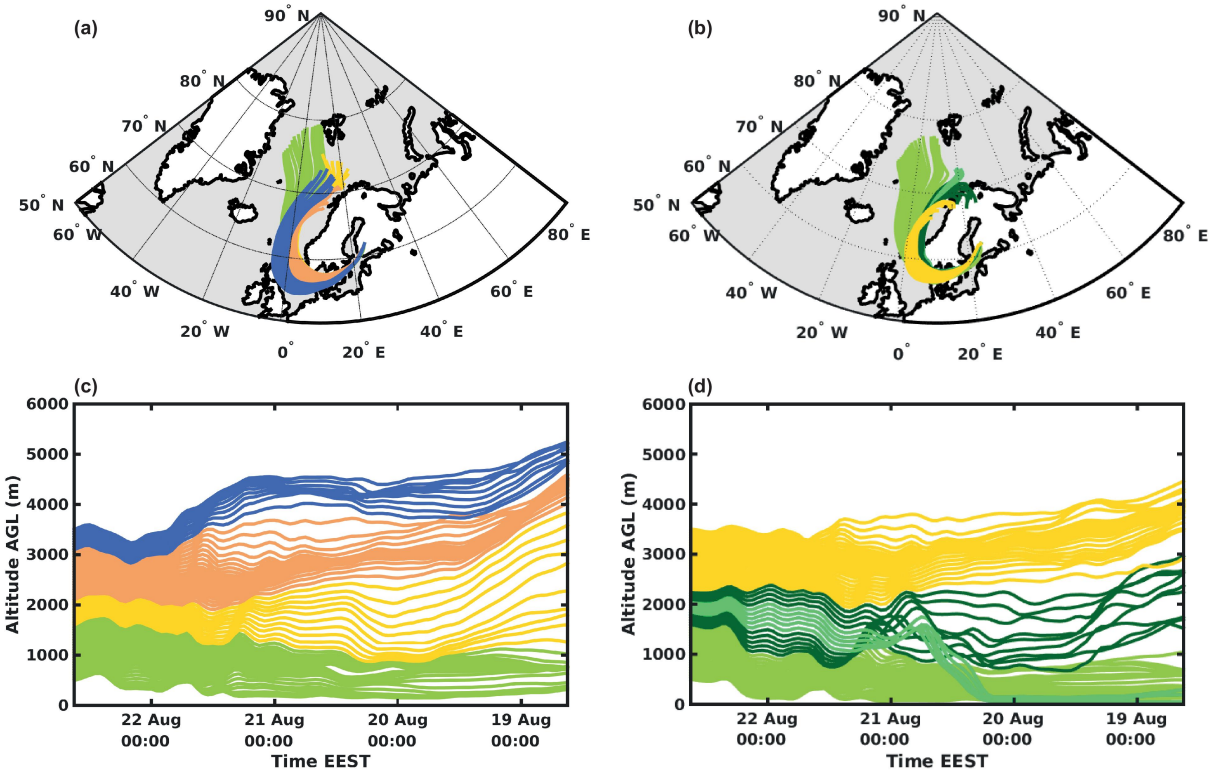

Figure 8: Same as Fig. 3 except for Case II with a), c) show trajectories arriving at 10:00 and panels b), d) at 14:00.

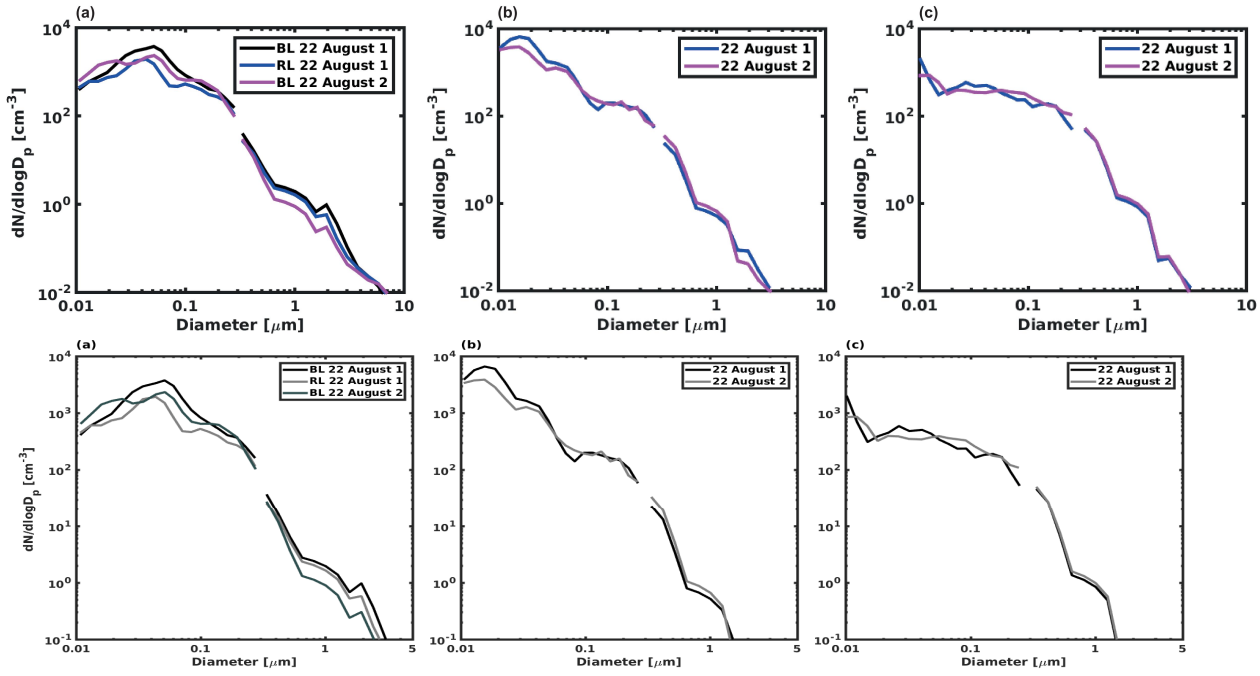

Figure 9: Evolution of the mean aerosol size distribution in Case II for a) boundary layer b) first middle layer and c) second middle layer.